

# **Non-covalent Assembly of Reversible Photoswitchable Surfaces**

By

---

Nipa Purohit

A Thesis submitted to the Faculty of the  
WORCESTER POLYTECHNIC INSTITUTE

In partial fulfillment of the requirements for the  
Degree of Master of Science

In

Chemistry

June 1, 2005

Approved:

---

Dr. W. Grant McGimpsey, Advisor

---

Dr. James P. Dittami, Department Head

## Abstract

Previous studies carried out in our laboratory resulted in the development of non-covalently assembled multilayered thin films incorporating metal ions such as Cu(II) and organic ligands including dicarboxypyridine. In one study, a SAM consisting of 4-[(10-mercaptodecyl)oxy]pyridine-2,6-dicarboxylic acid was deposited on gold. The pyridine group was then used to complex a layer of Cu(II) ions which in turn were capped by *cis*-2,2'-dipyridylethylene. This stilbene analog undergoes photoinduced *cis-trans* isomerization on the surface resulting in a substantial increase in the hydrophilicity of the surface leading to the possibility of creating virtual microfluidic valves and pumps. However, the photoswitchable wettability was irreversible. Stilbene-4,4-dicarboxylic acid was the ligand selected for generating a reversible system. The decision to use this stilbene moiety was based on molecular modeling and the commercial availability of both *cis* and *trans* forms. When 4-[(10-mercaptodecyl)oxy]pyridine-2,6-dicarboxylic acid was used as SAM, the stilbene-4,4'-dicarboxylic acid did not undergo photoisomerization. Prolonged irradiation leads to photodegradation of film. A mixed SAM of dodecanethiol and mercaptoundecanoic acid was used to create space on the surface and facilitate isomerization. But *cis-trans* isomerization of the stilbene moiety was not achieved by this system. When a mixed SAM of 4-[(10-mercaptodecyl)oxy]pyridine-2,6-dicarboxylic acid and 4-*tert* butylbenzenethiol was used, stilbene-4,4-dicarboxylic acid showed reversible photoinduced *cis-trans* isomerization for one complete cycle leading to a reversible change in wettability. After one cycle of isomerization the film photodegrades.

## Acknowledgement

I would like to express my deepest gratitude to my advisor Dr. W. Grant Mcgimpsey for his expert guidance, support and concern. Working in his research group was a great learning experience.

I would like to sincerely thank Dr. Christopher Lambert for his help and guidance with my research and would also like to appreciate his patience and effort while helping me with my thesis.

I would like to thank Prof. Venkat Thalladi and Prof. James Dittami for all their help and valuable advice.

Thanks to Dr. Christopher Cooper who taught me a great deal in the laboratory. Thanks to Nantanit Wanichacheva who has collaborated for a part of this research and who is also a good friend. Thanks to all my friends and colleagues Dr. Hubert Nienaber, Peter Driscoll, Ernesto Soto, Man Phewlaungdee, Eftim Milkani, Yasmin Shrivastava, Sara Strecker and Eugene Douglass. It was a great experience knowing you all and you all made my time at WPI very enjoyable.

Thanks to my friends Marta, Salim and Kasim for being there for me.

I would like to thank my parents and my sister for their love and support.

Most of all I would like to thank Chirag for his patience, unfailing support and encouragement.

Thanks to the many people who I might have not mentioned but who have made my stay at WPI memorable.

## Table of Contents

Abstract .....	2
Acknowledgement .....	3
Table of Contents .....	4
List of Figures .....	5
List of Tables .....	5
Introduction .....	8
Experimental .....	18
Materials .....	18
General Methods .....	18
Results and Discussion .....	24
1. Background .....	24
2. Selection of the ligand stilbene-4,4'-dicarboxylic acid .....	28
3. Studies done on stilbene-4,4'-dicarboxylic acid .....	31
4. Fabrication of film using 4-[(10-mercaptodecyl)pyridine-2,6-dicarboxylic acid as SAM .....	42
5. Fabrication of film using mixed monolayers of mercaptoundecanoic acid and dodecanethiol .....	54
6. Fabrication of film using mixed monolayers of 0.5mM 4-[(10-mercaptodecyl)pyridine-2,6-dicarboxylic acid and 0.5mM 4- <i>tert</i> butylbenzenethiol .....	58
Conclusion .....	70
References .....	71
Appendix A .....	75

## List of Figures

Figure 1. Self-assembly of surfactant in water to form a micelle	10
Figure 2. Self-Assembly of Biocidal Nanotubes from a single chain Diacetylene Amine salt	10
Figure 3. Preparation of SAM on gold	12
Figure 4. Non-covalent assembly of a multilayer film	13
Figure 5. Multilayer films used for generating photocurrent	14
Figure 6. Photoswitchable change in wettability	15
Figure 7. Switching wettability by electric potential	16
Figure 8. Structure of Film I and II. I can be converted to II by irradiating at 300nm	17
Figure 9. Schematic diagram for an ellipsometric measurement	23
Figure 10. Contact Angle Measurement	26
Figure 11. Cyclic voltammograms of bare gold and SAM on gold	26
Figure 12. <i>cis</i> of stilbene-4,4'-dicarboxylic acid	29
Figure 13. <i>trans</i> of stilbene-4,4'-dicarboxylic acid	29
Figure 14. Fabrication of film	30
Figure 15. IR spectra of <i>cis</i> and <i>trans</i> stilbene-4,4'-dicarboxylic acid	32
Figure 16. Absorption spectra of <i>cis</i> stilbene-4,4'-dicarboxylic acid and <i>trans</i> stilbene-4,4'-dicarboxylic acid	34
Figure 17. Absorption spectra of unirradiated <i>cis</i> stilbene-4,4'-dicarboxylic acid and irradiated <i>cis</i> stilbene-4,4'-dicarboxylic acid at 254nm.	35
Figure 18. Absorption spectra of <i>cis</i> stilbene-4,4'-dicarboxylic acid irradiated at 254nm (conversion to <i>trans</i> ) and this solution irradiated again at 350nm.	36
Figure 19. Absorption spectra of unirradiated <i>cis</i> stilbene-4,4'-dicarboxylic acid and irradiated <i>cis</i> stilbene-4,4'-dicarboxylic acid at 350nm.	37
Figure 20. Absorption spectra of unirradiated <i>trans</i> stilbene-4,4'-dicarboxylic acid and irradiated <i>trans</i> moiety.	38
Figure 21. Absorption spectra of <i>trans</i> stilbene-4,4'-dicarboxylic acid irradiated at 350nm (conversion to <i>cis</i> ) and this solution irradiated again at 254nm.	39
Figure 22. Absorption spectra of unirradiated <i>trans</i> stilbene-4,4'-dicarboxylic acid	

and irradiated <i>trans</i> stilbene-4,4'-dicarboxylic acid at 254nm.	40
Figure 23. Cyclic voltammograms obtained for bare gold, pyridine decanethiol on gold (SAM), and Cu/pyridine decanethiol on gold.	43
Figure 24. Cyclic Voltammograms of Cu/pyridine decanethiol on gold, Film III and Film IV	44
Figure 25. The grazing angle IR spectrum of a SAM of dicarboxypyridyl capped	48
Figure 26. The grazing angle IR spectrum of dicarboxy pyridyl SAM complexed with Cu(II) ions.	49
Figure 27. The grazing angle IR spectrum of SAM + Cu(II) ions + <i>cis</i> stilbene-4,4'-dicarboxylic acid	50
Figure 28. The grazing angle IR spectrum of Irradiated Film IV	51
Figure 29. IR spectra of Films IV, irradiated IV and SAM+ Cu	52
Figure 30. Fabrication of non-covalently assembled film using mixed SAMs of mercaptoundecanoic acid and dodecanethiol	54
Figure 31. IR spectra of irradiated Film V and mixed monolayer + Cu(II)+ <i>trans</i>	57
Figure 32. Fabrication of non-covalently assembled film using mixed SAMs (using <i>cis</i> form of stilbene-4,4'-dicarboxylic acid)	58
Figure 33. Fabrication of non-covalently assembled film using mixed SAMs (using <i>trans</i> form of stilbene-4,4'-dicarboxylic acid)	59
Figure 34. Variation in the values of contact angle as a function of the concentration of 4-[(10-mercaptodecyl)pyridine-2,6- dicarboxylic acid in solution.	60
Figure 35. Cyclic voltammograms obtained for bare gold, mixed monolayer on gold and Cu/mixed monolayer on gold, <i>cis</i> stilbene-4,4'-dicarboxylic acid on Cu	62
Figure 36. Cyclic voltammograms obtained for bare gold, mixed monolayer on gold and Cu/mixed monolayer on gold, <i>trans</i> stilbene-4,4'-dicarboxylic acid on Cu	62
Figure 37. Cyclic voltammograms obtained for mixed monolayers + Cu(II) and Film VII( <i>cis</i> form) and Film VII(irradiated)	63
Figure 38. Contact Angle Photos.	66
Figure 39. IR spectra of irradiated Film VII (at 254nm) and Film VIII	68
Figure 40. IR spectra of irradiated Film VII (at 254nm followed by irradiation at 350 nm) and Film VII	69

## List of Tables

<b>Table 1:</b> Contact angle measurements for Films III and IV	45
<b>Table 2:</b> IR assignments for Film IV and irradiated Film IV. (The individual layers are: (i)pyridine decanethiol (ii) Cu <sup>2+</sup> (iii) <i>cis</i> stilbene-4,4'-dicarboxylic acid (iv)Irradiated Film IV.	46
<b>Table 3:</b> IR assignments for Film III and irradiated Film III. (The individual layers are: (i)pyridine decanethiol (ii) Cu <sup>2+</sup> (iii) <i>trans</i> stilbene-4,4'-dicarboxylic acid (iv)Irradiated Film III.	47
<b>Table 4:</b> Contact angle measurements (Film V)	56
<b>Table 5:</b> Ellipsometric data for Film VII and Film VIII	61
<b>Table 6:</b> Contact angle measurements following the deposition of each layer of Film VII and after irradiation of Film VII	65
<b>Table7:</b> Contact angle measurements following the deposition of each layer of Film VIII and after irradiation of Film VIII	65

## Introduction

Nanotechnology is defined as the science of manipulating atoms and molecules to fabricate materials, devices and systems. Nanotechnology is not confined to any one particular scientific field but is of interest to all scientists whether they are physicists, chemists, biologists or engineers. Both the academic world and industrial world believe that the inception of nanotechnology has and will lead to improvement in industry, health and environment.

The word “nano” is derived from the Greek word “*nanos*” which means dwarf. In general terms, nanotechnology is defined as the technology dealing with matter on a molecular size scale of nanometers ( $10^{-9}$ m). According to the Oxford English Dictionary, the term “nanotechnology” was coined in 1974 but it was first conceptualized in 1959 by Richard Feynman<sup>(1)</sup>. Feynman proposed a link between biology and manufacturing and asked people to consider how the biological cells manufacture substances on an extremely small scale and also store information. In his famous talk given at the annual meeting of the American Physical Society held at the California Institute of Technology (Caltech),<sup>(1)</sup> he urged people “to consider the possibility that we, too, can make a thing very small, which does what we want—that we can manufacture an object than maneuvers at that level.”

For the fabrication of nanometer scale devices two different approaches, “top down” approach and “bottom up” approach are used. The basic principle behind “Top

down” approach is to make existing devices so small that they eventually finish up as nanosized objects, with dimensions of not more than a few hundred nanometers. “Top down” approach typically uses etching techniques. A common example of the “top down” approach is the manufacturing of transistors on computer chips. The "top down" approach is time consuming and it limits the amount of bulk fabrication. It does have excellent precision but this is at the expense of rapid fabrication.

The “bottom-up” approach, involves constructing nanodevices from their constituent parts, i.e. atoms or small molecules. This approach tries to mimic nature. In nature materials are built from the “bottom up”, one atom or molecule at a time. These materials include inorganic minerals, pearls, bone and teeth, wood, silk etc. Fabrication by “bottom up” approach is achieved by either physical relocation of the building blocks into their required locations, or by using molecular self-assembly. The former route involves techniques such as the use of laser tweezers or atomic force microscopy. This process is difficult and molecules occasionally stick to the substrate and break apart. Molecular self-assembly is defined as the spontaneous organization of molecules into well-defined aggregates. Molecular self-assembly occurs because it is the lowest energy structure and therefore the most stable. The two key elements for molecular self assembly are chemical complementarities and structural compatibility through weak and non-covalent interactions. Figures 1 and 2 show such self-assembled systems. Generation of self-assembled systems is not time consuming.

**Figure 1.** Self-assembly of surfactant in water to form a micelle (due to the hydrophobic and hydrophilic interactions with water)

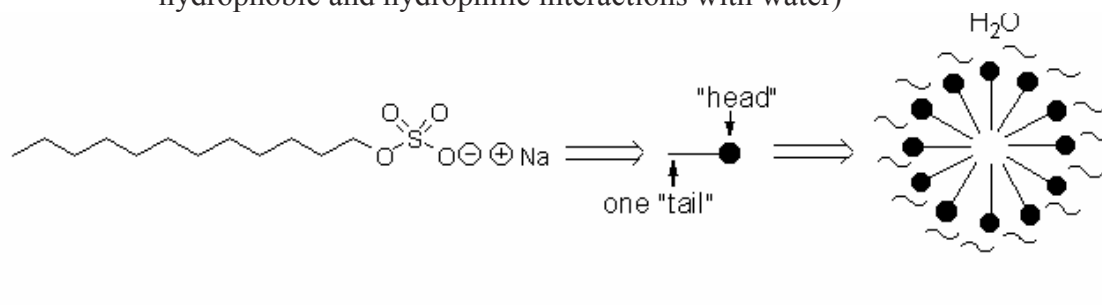
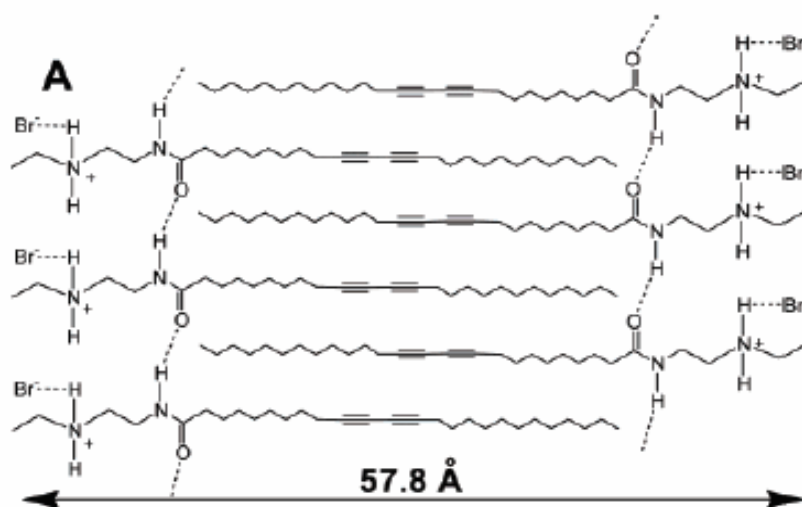
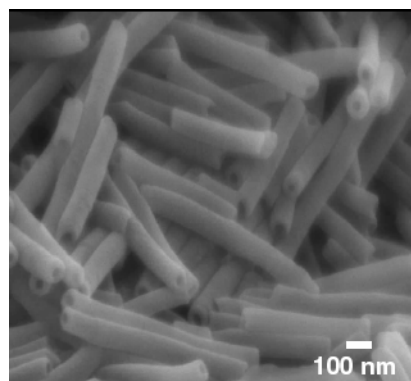


**Figure 2.**<sup>(2)</sup> Self-Assembly of Biocidal Nanotubes from a single chain Diacetylene Amine salt (as a result of H-bonding)

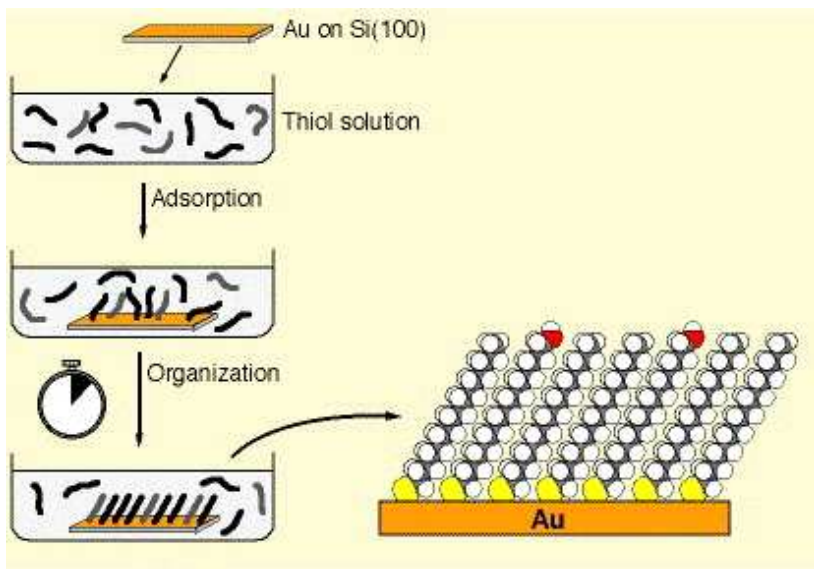


↓  
Self assembles to form nanotubes



Organic monolayer films also known as thin films have been prepared mainly by using Langmuir-Blodgett techniques<sup>(3,4)</sup> or by formation of self- assembled monolayers (SAMs). In the Langmuir- Blodgett technique a film assembled at an air-water interface is transferred to a solid substrate. Formation of SAMs takes place by spontaneous adsorption of the film components from a solution to the surface. SAMs of chlorosilanes on silicon<sup>(5,6)</sup> and organosulfur<sup>(7-9)</sup> compounds on gold are well known. Langmuir-Blodgett films have certain commercial applications but the films are not very robust. In 1983, Nuzzo and Allara reported the formation of monolayers of dialkyl disulfides on gold.<sup>(7)</sup> Sulfur has a natural affinity for gold<sup>(10)</sup> and when a clean gold slide is immersed in a solution containing alkanethiols, self-assembly takes place rapidly. The chemistry of sulfur compounds is well known and so it is possible to functionalize the monolayers. Alkanethiols form densely packed, well-ordered monolayers on gold.<sup>(9,11)</sup> A gold surface comprises of thin gold films on flat supports, typically glass or silicon. A schematic outline of the SAM preparation procedure on gold substrates is given in Figure 3. As shown in the figure when the substrate, gold on Si, is immersed in a solution of desired alkanethiols initial adsorption of the thiol is fast which is followed by slow organization of the molecules on the surface.

**Figure 3.** Preparation of SAM on gold (<http://www.ifm.liu.se/applphys/ftir/sams.html>)



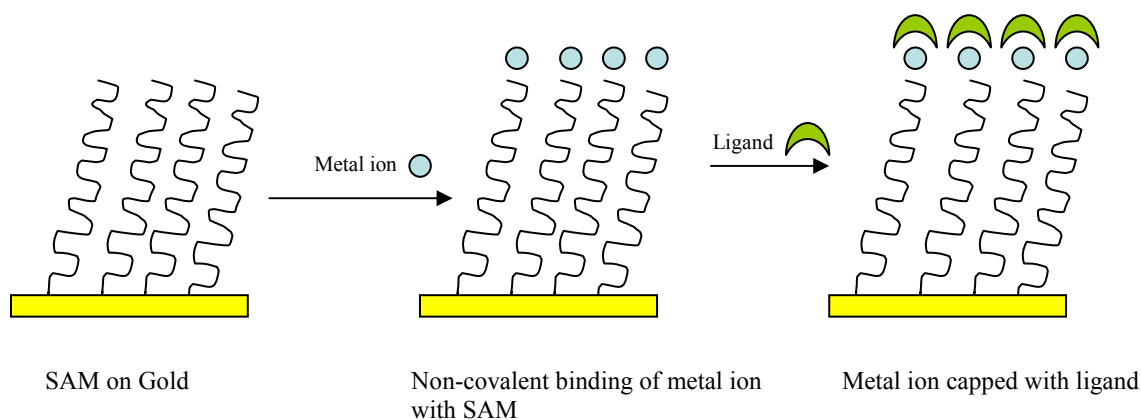
The Au-thiolate bond has bond strength of 44 kcal/mol and contributes to the stability of the SAMs together with the van der Waals forces between adjacent methylene groups. Monolayers on gold are stable in various solvents and also in the presence of light or under sonication.<sup>(12)</sup> High degree of order, stability and the possibility to modify the surface by chemically modifying the alkanethiols make the SAMs of alkanethiols on gold a very useful system for studies in physical, chemical and biological sciences.

Multicomponent SAMs, also known as mixed monolayers are useful in studying the phenomena of wetting,<sup>(13,14)</sup> adhesion,<sup>(15)</sup> electron transfer<sup>(16,17)</sup> and devices and sensors.<sup>(18)</sup> Mixed monolayers can be formed by exposing the gold surface to a solution containing a mixture of thiols. The surface composition of the resulting mixed monolayer may or may not be similar to the composition of the solution from which it was formed. The coadsorption of thiols is the general method for generating mixed monolayer films

which can have different chain lengths and also different terminating functional groups. However, factors governing the formation of mixed monolayers are not well understood.

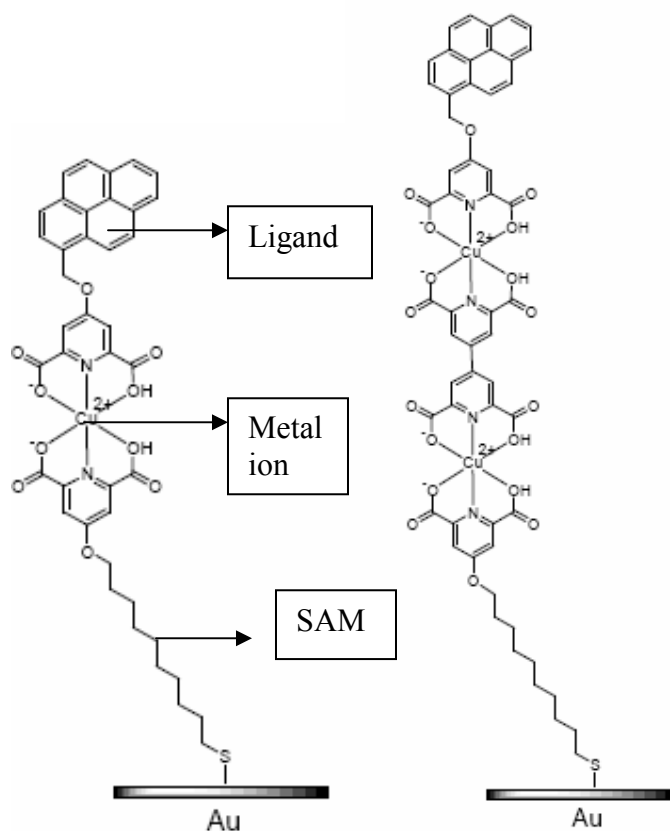
Synthesis of thiols with desired functional groups may sometimes prove to be laborious and time consuming. To overcome this difficulty, multilayer films which can be fabricated using non-covalent interactions between SAMs and metal ions have been developed. Multilayer films developed previously by Ulman (mercaptoalkanoic acid and copper ions)<sup>(19)</sup> and Bard (alkanedithiols acid and copper ions)<sup>(20)</sup> lacked stability. Dr. Christopher Cooper and Ernesto Soto of this laboratory came up with the approach of fabricating a stable non-covalently bound multilayer films on gold surfaces using 4-[(10-mercaptodecyl)pyridine-2,6-dicarboxylic acid as SAM and copper ions. These films were stable and easy to fabricate.<sup>(21,22)</sup> (Figure 4). The multilayer films can help control the molecular architecture and chemical and physical properties of layered assemblies on surfaces.

**Figure 4.** Non-covalent assembly of a multilayer film



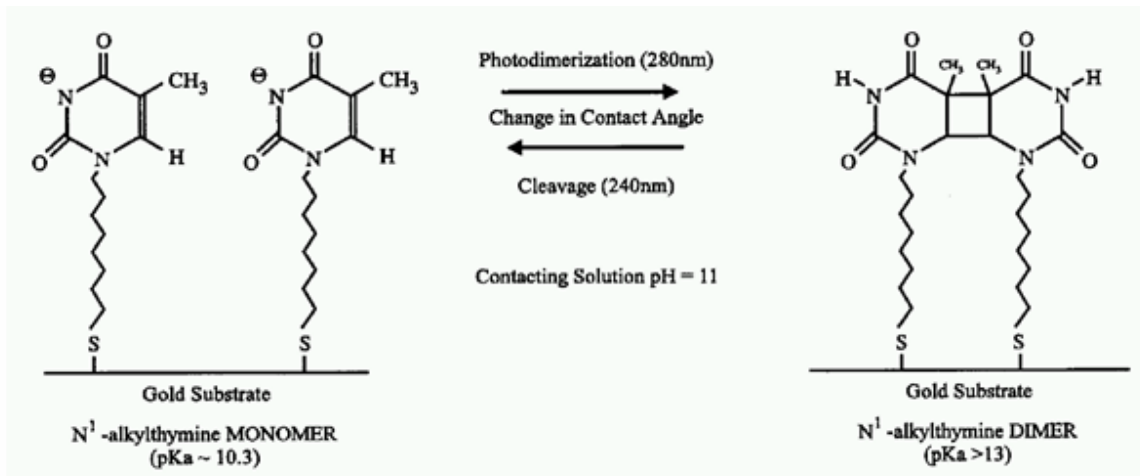
The multilayer films were fabricated by self-assembly of 4-[(10-mercaptodecyl)pyridine-2,6-dicarboxylic acid on a clean gold surface. This was followed by the deposition of Cu(II) ions that complex with the head group of the previous layer, and finally, deposition of a ligand which non-covalently binds to the Cu(II) ions as shown in Figure 5. The selection of the ligand is governed by the function desired from the multilayer film. The metal ion can also be changed depending on the choice of ligand. This approach has been used to fabricate films that conduct charges and that can change wettability upon irradiation.

**Figure 5.** <sup>(21)</sup> Multilayer films used for generating photocurrent



The properties of a surface like wetting, electron transfer and biocompatibility can be controlled by controlling behavior of the SAMs. There is lot of interest in generating controlled surfaces also known as “smart surfaces”. Smart surfaces are defined as surfaces whose properties can be regulated in response to external stimuli. The external stimuli can be light, solvent, pH, temperature or electric potential. Smart surfaces with switchable surface properties can prove very important for information storage, for constructing microfluidic devices, biosensors and so on.<sup>(23-25)</sup> Figures 6, 7 and 8 depict such smart surfaces.

**Figure 6.**<sup>(26)</sup> Photoswitchable change in wettability



As shown in Figure 6, on irradiation with UV light at 280nm and 240nm, the SAM of long-chain thymine-terminated thiols gives a contact angle change of 26°. As the contacting solution used here has pH = 11.1 the monomer is ionized. The contact angle change occurs upon dimerization due to the decrease in surface charge.

**Figure 7.** Switching wettability by electric potential

([http://web.media.mit.edu/~manup/papers/SiBio\\_pres.ppt#266,11,Method](http://web.media.mit.edu/~manup/papers/SiBio_pres.ppt#266,11,Method))

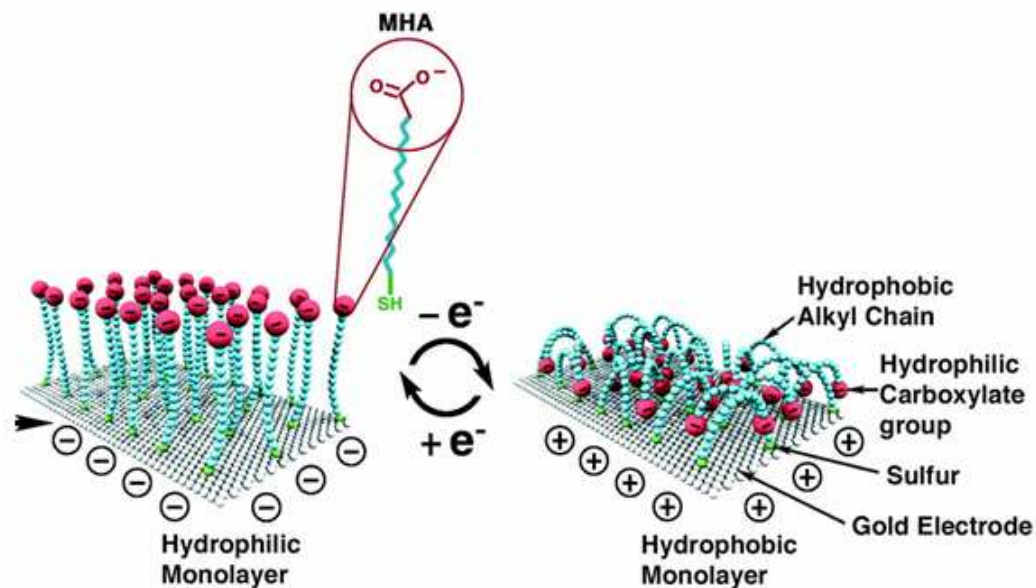
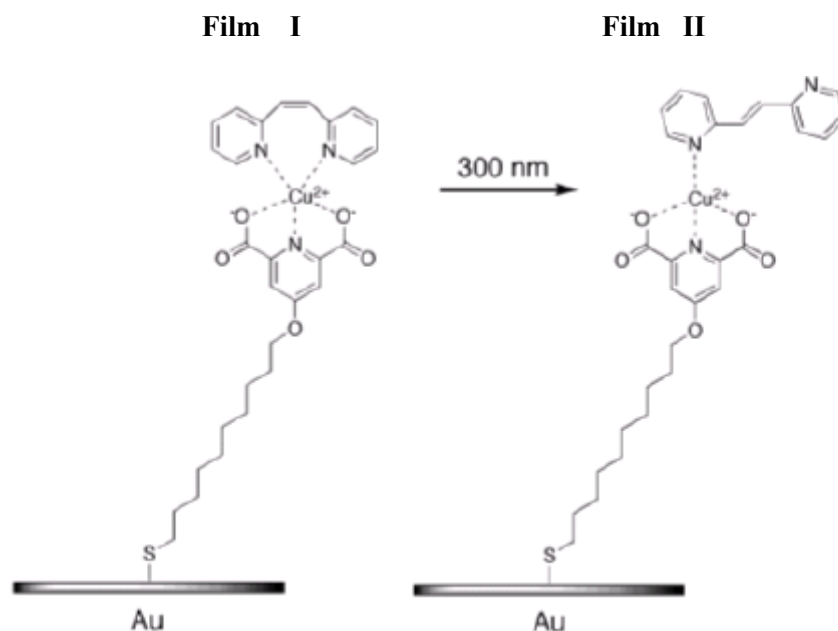


Figure 7 shows reversible conformational behavior of 16-mercaptohexadecanoic acid (MHA) under positive and negative potential. Changes in potential lead to the change in wettability.<sup>(27)</sup>

This laboratory has had considerable success in controlling the wettability of the surface by using non-covalently fabricated multilayer systems described earlier.<sup>(22)</sup> The multilayer system shown in Figure 8 was developed to control the wettability of the surface. The ligand used was an isomerizable compound 2,2'-dipyridylethylene.<sup>(22)</sup>

**Figure 8.**<sup>(22)</sup> Structure of Film I and II. I can be converted to II by irradiating at 300nm



Deposition of *cis* and *trans*-2,2'-dipyridylethylene lead to differences in the surface wettability with the *cis*-isomer providing a more hydrophobic surface as was determined from contact angle measurements. The irradiation of Film I at 300nm lead to a decrease in contact angle of  $\sim 19^\circ$ . However this change in contact angle was found to be irreversible.

The goal of this thesis was to fabricate a non-covalently assembled system which was reversible and also gave a substantial change in contact angle.

## Experimental

### **Materials.**

All materials were used as received without further purification. Unless otherwise noted, reagents and solvents were purchased from Sigma-Aldrich, (Wisconsin, USA.) *cis* - stilbene-4,4'-dicarboxylic acid was purchased from Lancaster Synthesis Inc. (New Hampshire, USA). *trans*-Stilbene-4,4'-dicarboxylic acid was purchased from Frinton Laboratories, (New Jersey, USA). Gold slides were purchased from Evaporated Metal Films Inc. (EMF), (New York, USA.) 4-[(10-mercapto)decyl]pyridine-2,6-dicarboxylic acid was synthesized by Dr. Christopher Cooper in this laboratory.<sup>(21,22)</sup>

### **General Methods.**

#### **i. NMR**

Proton nuclear magnetic resonance (<sup>1</sup>H NMR) spectra were obtained on a Bruker AVANCE 400 (400 MHz) NMR spectrometer. Chemical shifts are reported in ppm (δ) relative to tetramethylsilane (TMS).

## **ii. UV-Visible Spectroscopy**

Absorption spectra were recorded using a quartz cuvette (1cm x 1cm) with a Perkin-Elmer Lambda 35 UV Spectrophotometer. The lamps used for irradiation of solutions were 254nm Rayonet lamp and 350 nm Rayonet lamp. The lamp profiles for both the lamps are given in Appendix A.

## **iii. Computational Studies**

Molecular structures were minimized for energy using the Molecular Operating Environment (MOE), version 2000.02 computing package (Chemical Computing Group Inc., Montreal, Quebec, Canada.). Structures were minimized first using the AMBER94 potential control under a solvent dielectric of 24. Minimized structures were then subjected to a 30-ps molecular dynamics simulation employing the NVT statistical ensemble. Dynamics calculations on structures were heated to 400 K, equilibrated at 310 K and cooled to 290 K at a rate of 10 Kelvin/picosecond. The lowest energy structures obtained from these calculations were re-minimized for energy.

## **iv. SAM and Multilayer Preparation.**

The dimensions of gold slides were 25 mm x 75 mm x 1 mm. Each slide is coated with 50 Å of Cr followed by 1000 Å of Au.. Based on the experiment to be carried out the gold slides were cut into different sizes. In order to remove any adsorbed impurities the gold slides prior to use were immersed in piranha solution (70% sulfuric acid, 30% hydrogen peroxide (30% aqueous)) at 90° C for 20 minutes.<sup>(28)</sup> After removing the slides

from the piranha solution they were washed with deionized water, dried with nitrogen, and used immediately. Monolayers were prepared by immersion of the clean gold slides in a 1-2 mM solution of 4-[(10-mercaptodecyl)oxy]pyridine-2,6-dicarboxylic acid in ethanol for 12 hours.<sup>(21,22)</sup> Mixed monolayers were prepared by immersing the clean gold slides in a solution containing ethanolic solutions of 0.7mM mercaptoundecanoic acid and 0.3mM dodecanethiol. A different type of mixed monolayers were prepared by immersing the clean gold slides in a solution containing a mixture of 0.5mM of 4-[(10-mercaptodecyl)oxy]pyridine-2,6-dicarboxylic acid and 0.5mM of 4-*tert* butylbenzenethiol in ethanol (for mixed monolayers the total concentration of thiol was 1mM). Copper (II) bromide was used as the source of Cu (II) ions. The SAM covered gold slides were immersed in a solution of 1mM Copper bromide in ethanol. Complete complexation of Cu (II) ions with the SAM was reached after 3 hours of submersion.<sup>(22)</sup> Capping of the copper ions with the *cis* and *trans* stilbene-4,4-dicarboxylic acid was carried out by immersing the copper capped gold slides in 5 mM solutions in ethanol. Coverage was completed after 36-48 h of exposure. To determine the coverage time the contact angle, cyclic voltammogram and infrared spectrum were recorded after every 4 hours. After every deposition, the films were thoroughly rinsed with ethanol in order to remove any physisorbed species, and dried under nitrogen. In the mixed monolayer systems following deposition of Cu (II) the gold slides were submersed in a solution of 2N HNO<sub>3</sub> for 30 minutes and then rinsed with water followed by ethanol to remove the any copper ions that may have physisorbed on CH<sub>3</sub> head group.

**v. Cyclic Voltammetry.**

All electrochemical experiments were carried out with an EG&G Princeton Applied Research Potentiostat/Galvanostat Model 273. A three-electrode setup was used with the gold slide as the working electrode, a saturated calomel electrode (SCE) as the reference electrode, and platinum wire as the counter electrode. Electrical contact was made to the gold slide by means of an alligator clip. The solution used for the experiments was aqueous solution of 1mM potassium ferricyanide with 50mM potassium chloride as a supporting electrolyte. The area of the gold slide dipped in the solution was about 1cm<sup>2</sup>. To reduce electrical noise, the electrochemical cell was placed inside a Faraday cage. The cyclic voltammetry curves were obtained in the range of -0.06 to +0.7 V, with a scan rate of 50mV/s and a scan increment of 1mV.

**vi. Contact Angle Measurements.**

Contact angle measurements were obtained with a Rame-Hart Model 100-00 Goniometer. To measure the contact angle made by water with the surface, one micro liter droplet of water (pH ~ 5.5, not buffered) was added to the slide using a calibrated micro pipette. On one slide about five measurements were recorded for five different droplets. Contact angle was measured immediately after each droplet was added. The value of contact angle for each sample was an average of 15-20 measurements from 15-20 drops. Standard deviation was calculated for each sample.

**vii. Infrared spectroscopy.**

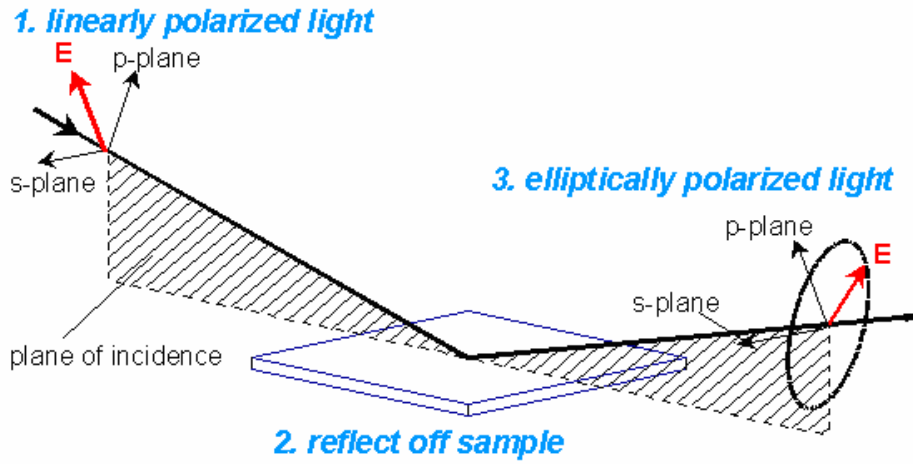
IR spectra for the SAMs were obtained on a Nexus FT-IR spectrometer equipped with a ThermoNicolet grazing angle accessory and a liquid-nitrogen cooled MCTA detector. The IR beam was incident at  $75^\circ$  on the gold substrates. The optical path was purged with nitrogen gas before and during data acquisition. Before every sample run a background spectrum was collected from a clean, bare gold slide. For each sample, 64 scans were collected with a  $4\text{ cm}^{-1}$  resolution. The scan range was from  $4000$  to  $600\text{ cm}^{-1}$ , although the detector sensitivity falls off below  $1000\text{ cm}^{-1}$ . Therefore, peaks appearing below  $1000\text{cm}^{-1}$  were not used for characterization of the film on the gold slide.

IR spectra for solid samples were obtained using a Nexus FT-IR spectrometer equipped with Attenuated Total Reflectance (ATR) accessory.

**viii. Ellipsometry.**

Ellipsometric measurements were carried out on a Rudolph manual ellipsometer using a wavelength of  $6328\text{ \AA}$  (He-Ne laser) and an incident angle of  $70^\circ$ . Three to five separate points were measured on each sample and the range was found. A refractive index of 1.45 was assumed for the monolayer. Ellipsometry uses polarized light to characterize thin films. Figure 9 shows the basic principle behind Ellipsometry.

**Figure 9.** Schematic diagram for an ellipsometric measurement (<http://www.jawoollam.com>)



Linearly polarized light is incident on the surface. This light interacts with the sample and reflects from it. The interaction of the light with the sample changes the linearly polarized light to elliptically polarized light. The polarization change is measured by analyzing the light reflected from the sample. The ellipsometer has two polarizers. The first polarizer is used to generate linearly polarized light and the second polarizer which is known as the analyzer measures the output polarization state. The sample is placed in between the two polarizers. The polarization change is given by two values  $\Psi$  and  $\Delta$  that describe this polarization change and they are related to the ratio of Fresnel reflection coefficients  $R_p$  and  $R_s$  for  $p$ -(parallel) and  $s$ -(perpendicular) polarized light, respectively.

$$\rho = \tan (\Psi) e^{i\Delta} = R_p/R_s$$

$\Psi$  and  $\Delta$  are functions of optical constants ( $n$  – refractive index and  $k$ - extinction coefficient) and film thickness. Film thickness and optical constants are found from the values of  $\Psi$  and  $\Delta$  using Fresnel Reflection Coefficients and Snell's law.

# Results and Discussion

## 1. Background

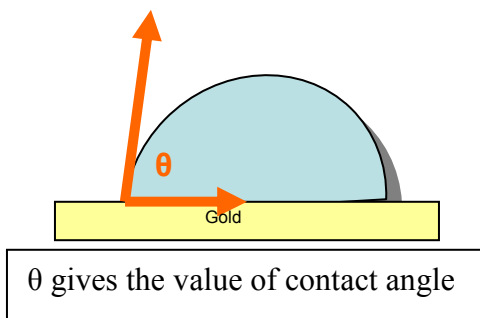
Multilayer films were fabricated by the non-covalent assembly of 4-[(10-mercaptodecyl)pyridine-2,6-dicarboxylic acid on a clean gold surface, followed by the deposition of Cu(II) ions that complex with the head group of the previous layer, and finally, deposition of the ligand stilbene-4,4'-dicarboxylic acid which serves to cap the Cu(II) ions. This assembly was based on the fabrication of non-covalent systems described in the introduction<sup>(21,22)</sup> (Figure 4). The deposition of each layer is followed using Grazing Angle IR, Contact Angle Measurements, Cyclic Voltammetry and Ellipsometry.

Functional group identification in monolayers can be achieved by using grazing angle IR spectroscopy. This technique can determine the presence of each successive layer in a multilayer film as they are deposited.<sup>(21,22)</sup> Grazing angle IR Spectroscopy has also been used to study the packing of monolayers on gold and the contributions of chain orientation and chain lengths. IR spectroscopy was used as the main characterization technique by Porter et al. to show that that long-chain thiols form a densely packed, crystalline-like assembly with fully extended chains tilted from the surface normal by 20°-30°.<sup>(9)</sup> Characterization carried out using IR spectroscopy<sup>(29,30)</sup> for SAMs of alkanethiols suggest that the positions of the -CH<sub>2</sub> stretching modes are indicative of the extent of lateral interaction between the long n-alkyl and polymethylene chains and are sensitive to the crystallinity<sup>(10,31-34)</sup> of the thin films. For SAMs of alkanethiols the

presence of a  $\text{-CH}_2$  asymmetric stretching ( $\nu_a$ ) peak at  $2918\text{cm}^{-1}$  indicates a crystalline like assembly of the long chain thiols on the surface<sup>(9)</sup> and quasi-crystalline packing arrangements is indicated by a shift in the asymmetric  $\text{-CH}_2$  stretch in the IR to  $\sim 2925\text{ cm}^{-1}$ .<sup>(12)</sup> Thus IR spectroscopy, along with providing functional group identification gives an idea about the order on the surface.

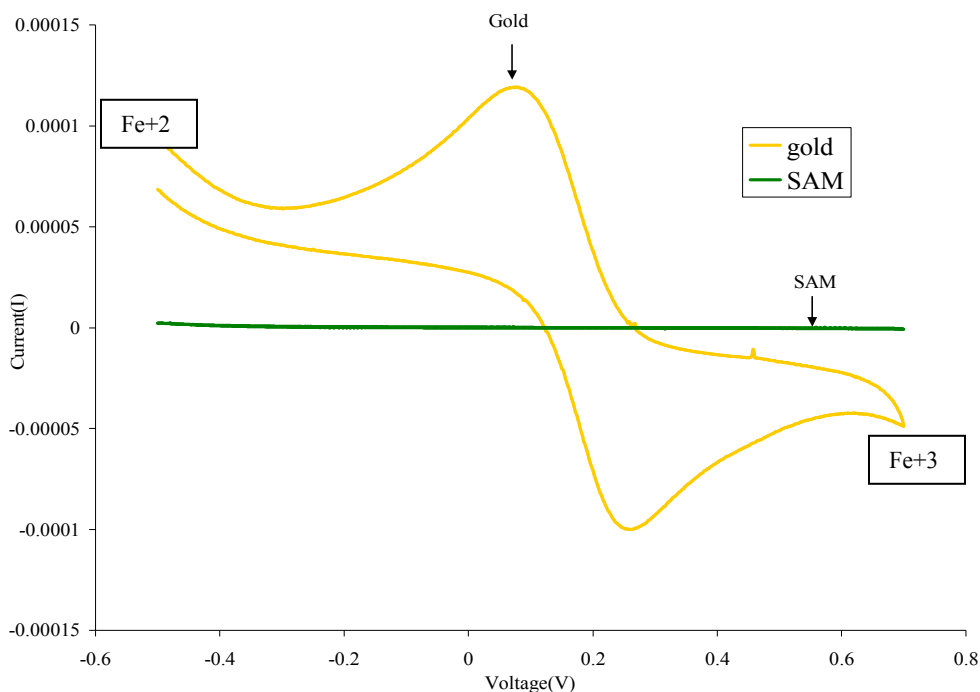
The contact angle of water on a thin film is measured using a goniometer. It is a well known and widely used technique for studying the wetting behavior of surfaces.<sup>(8,35-38)</sup> For contact angle measurement a small drop of water ( $1\ \mu\text{L}$ ) is placed on the SAM. The angle formed between the water droplet and the substrate provides information as to the hydrophilic or hydrophobic character of the surface (Figure 10). Decrease in the value of contact angle indicates increase in hydrophilicity of the surface and increase in the value of contact angle indicates increase in hydrophobicity. As the interaction between the thiol and gold is very strong (bond strength between gold and sulfur is  $\sim 44\text{kcal/mole}$ ), many functional groups can be included as a part of the monolayer without changing the adsorption of the thiol group to the gold surface. Contact angle measurements have shown that adsorption of n-alkanethiols generates highly hydrophobic surfaces and the alcohol or carboxylic acid terminated thiols generates hydrophilic surfaces.<sup>(8)</sup> Thus contact angle measurements have proved that terminal groups like  $\text{-OH}$ ,  $\text{-COOH}$  etc. are located at the outer surface.<sup>(8,39-41)</sup>

**Figure 10.** Contact Angle Measurement



Cyclic voltammetry is used for studying the formation of monolayer. The cyclic voltammogram(CV) of a bare gold surface in a solution of potassium ferricyanide shows the redox peaks of the ferricyanide.<sup>(42)</sup> Formation of SAM on the gold makes the gold insulating and results in the decrease in current in the CV redox wave.<sup>(43-49)</sup> The complete disappearance of the redox wave indicates the formation of a well ordered monolayer (Figure 11).

**Figure 11.** Cyclic Voltammograms of bare gold and SAM on gold



The thickness of a monolayer is measured using Ellipsometry.<sup>(8,50-53)</sup> The thickness of a monolayer varies with the variation in chain length of the monolayer. In the case of a multilayer the value of thickness increases with deposition of successive layers.

## 2. Selection of the ligand stilbene-4,4'-dicarboxylic acid

This laboratory has had considerable success in controlling the wettability of the surface by using non-covalently fabricated multilayer systems.<sup>(22)</sup> A system which was both reversible and gave a substantial change in contact angle was desired. The decision to use stilbene-4,4'-dicarboxylic acid as a ligand to cap Cu(II) ions in the multilayer was based on the demonstrated success of the strategy of non-covalent fabrication of multilayers. As the film had to be fabricated using metal-ligand interactions, the ligand needed to have a group which could bind with the metal ion and also have a polar group which would help change the wettability of the surface. Moreover as light was to be used as the stimuli for changing the surface wettability the ligand had to be photoisomerizable. Molecular modeling was done for *cis* and *trans* stilbene-4,4'-dicarboxylic acid. Figure 12 shows the molecular model of the *cis* form and Figure 13 shows the model of the *trans* form. If *cis* stilbene-4,4'-dicarboxylic acid was used as the ligand and if the ligand would bind to the Cu(II) ions through one of the –COOH groups then as depicted by Figure 12 (model of the *cis* form) the hydrophobic part of the ligand would be exposed to the surface. If the *trans* form was used as the ligand and if it would binds to the Cu(II) ions through one of the –COOH groups then as depicted by Figure 13(model of the *trans* form) the hydrophilic part of the ligand would be exposed to the surface. Moreover both *cis* and *trans* forms of stilbene-4,4'-dicarboxylic acid are commercially available making it an ideal ligand for our multilayer system. Fabrication of the multilayer is shown in Figure 14. Film III (*trans* form- hydrophilic surface) and Film IV (*cis* form- hydrophobic

surface) demonstrate how the surface wettability might be controlled by photoisomerization.

**Figure 12.** *cis* stilbene-4,4'-dicarboxylic acid

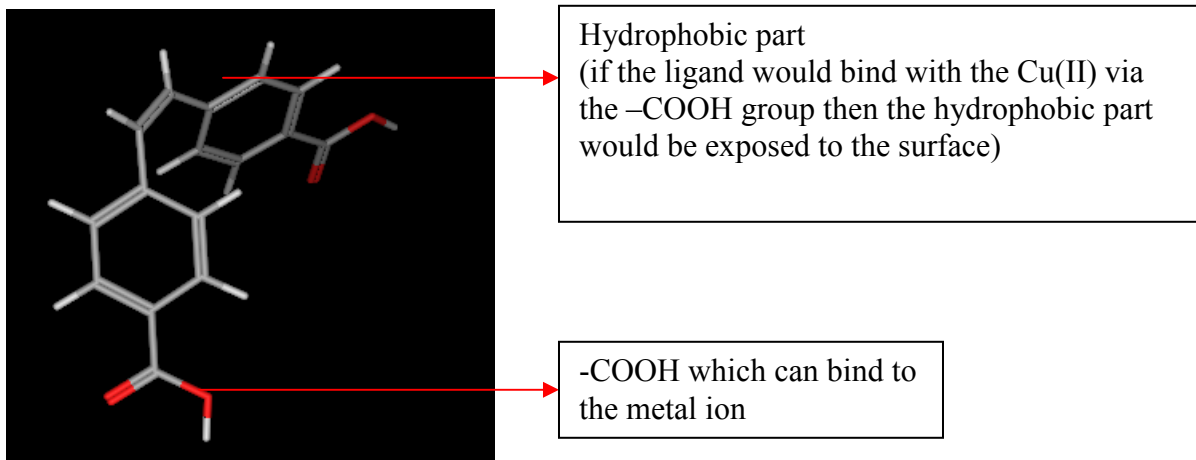


**Figure 13.** *trans* stilbene-4,4'-dicarboxylic acid

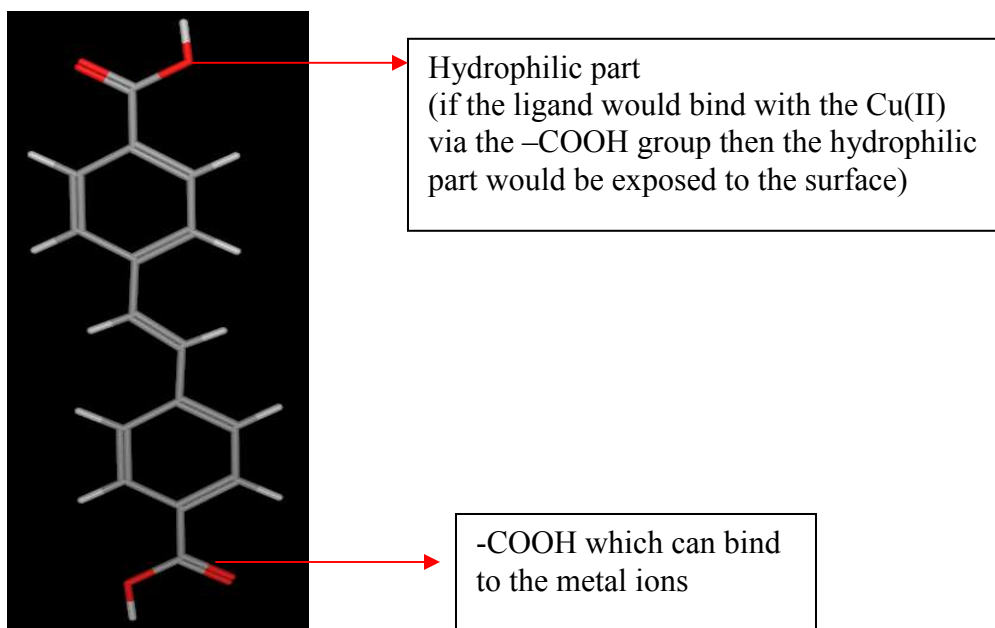
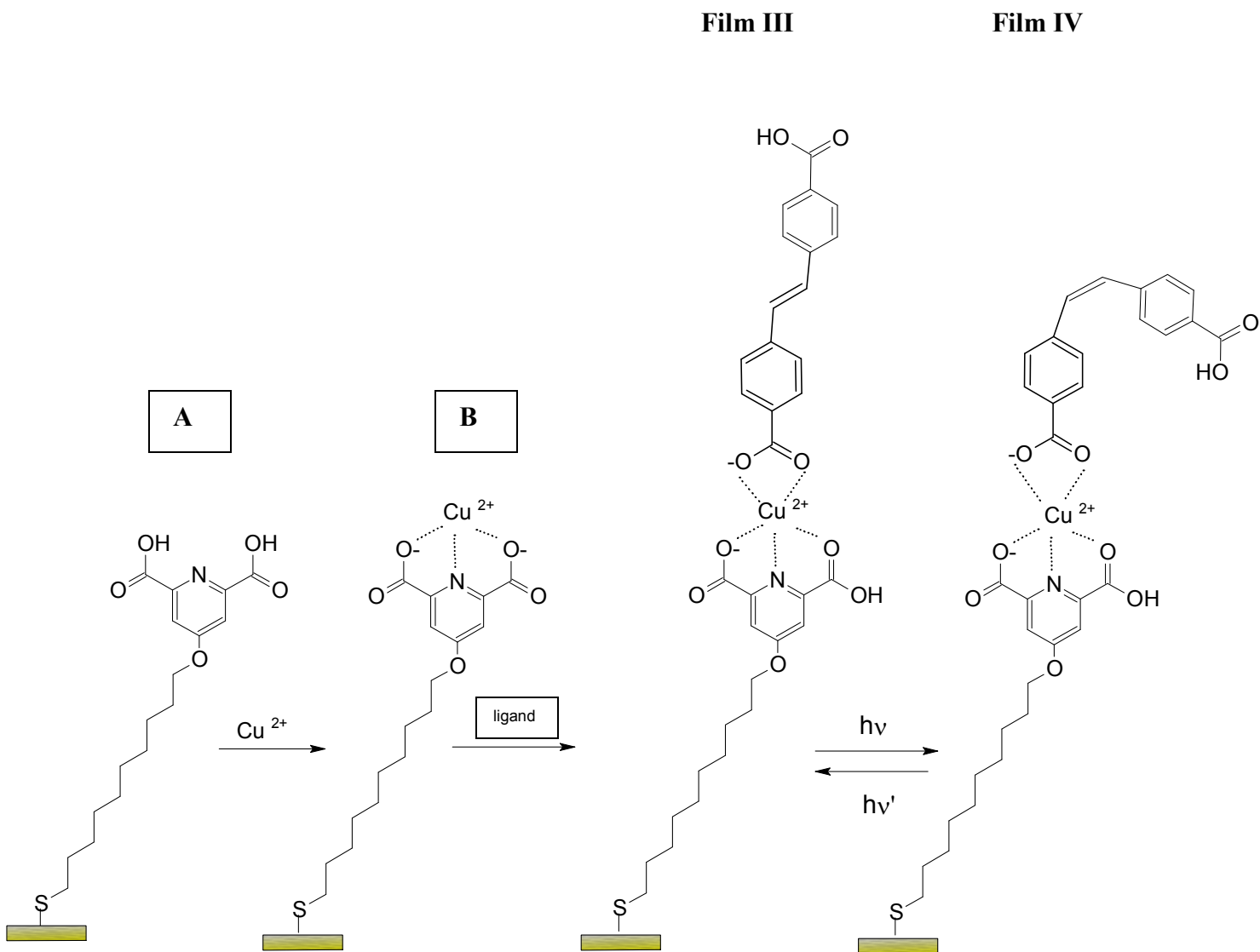


**Figure 14.** Fabrication of film

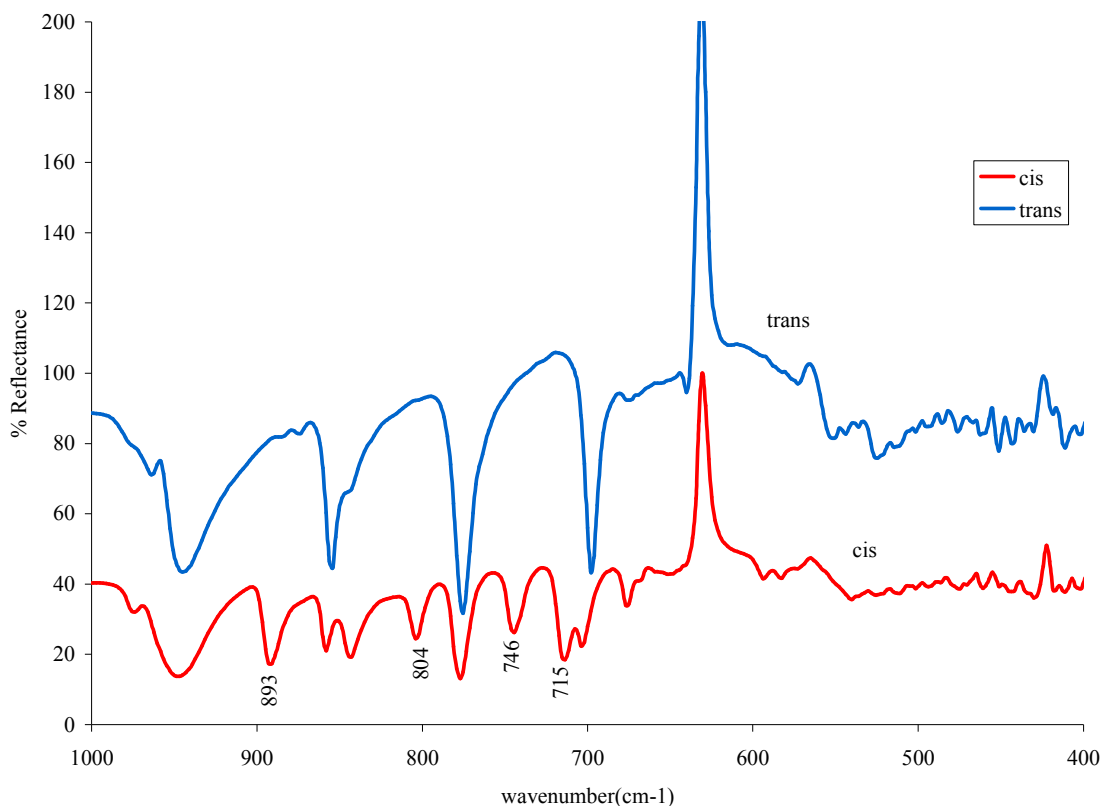


### 3. Studies done on stilbene-4,4'-dicarboxylic acid

Photochromic molecules are known to behave differently on surfaces as compared to solution.<sup>(54)</sup> Stilbene and derivatives of stilbene can undergo photoprocesses like isomerization, cyclization, dimerization and excimer formation. These processes occur to different extents depending on the environment. NMR and fluorescence studies have revealed that the photochemistry of stilbenes derivatives in solid state and micelles is quite different than that observed in solution.<sup>(55-58)</sup> In solid state, dimerization and excimer fluorescence are usually dominant whereas isomerization and monomer fluorescence are dominant in solutions. The photoisomerization properties of stilbene-4,4'-dicarboxylic acid in solution have been used as a guideline for the study on gold surfaces. The stilbene moiety was studied using FT-IR, NMR, UV-Vis spectroscopy.

The IR spectra of solid *cis* and *trans* stilbene-4,4'-dicarboxylic acid were obtained using ATR spectroscopy. Any significant difference between the IR spectra of the solid *cis* and *trans* isomers can be seen only below  $1000\text{cm}^{-1}$ . Figure 15 shows the difference in the spectra between the solid *cis* and *trans* compounds. The *cis* compound shows peaks at  $893\text{cm}^{-1}$ ,  $804\text{cm}^{-1}$ ,  $746\text{cm}^{-1}$  and  $715\text{cm}^{-1}$ . These peaks are absent in the spectra of the *trans* compound. The remaining IR spectra are given in Appendix A.

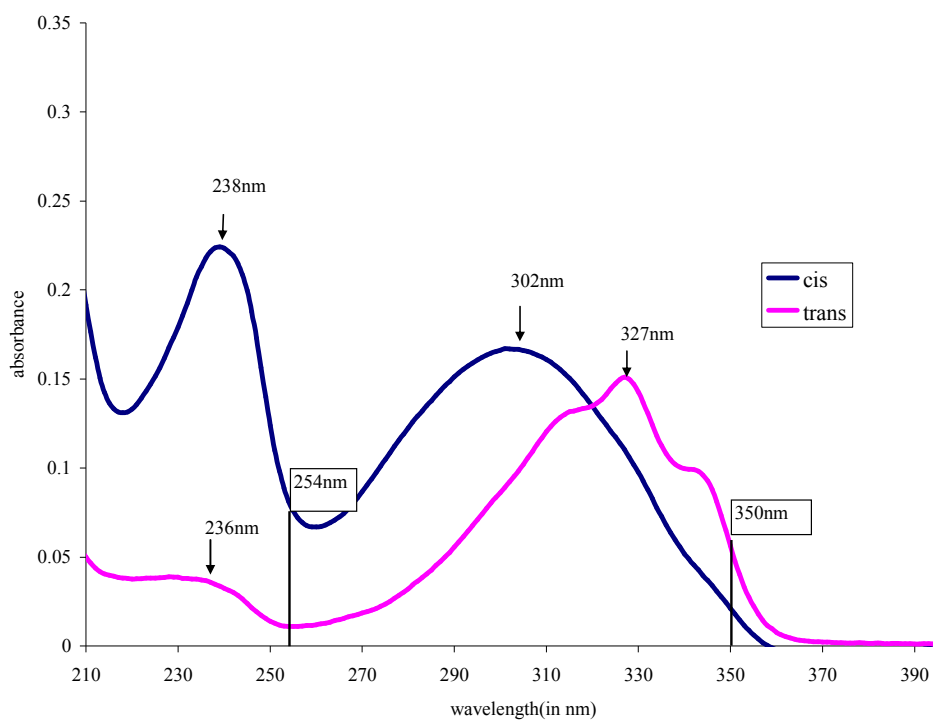
**Figure 15.** IR spectra of *cis* and *trans* stilbene-4,4'-dicarboxylic acid (from 1000-400  $\text{cm}^{-1}$ )



The photoinduced isomerization of *cis* and *trans* stilbene-4,4'-dicarboxylic acid in ethanol solution was observed by a UV-VIS spectrophotometer. The absorption spectra of *cis* stilbene-4,4'-dicarboxylic acid and *trans* stilbene-4,4'-dicarboxylic acid are given in Figure 16. An ethanolic solution of *cis* stilbene-4,4'-dicarboxylic acid ( $10^{-5}\text{M}$ ) was irradiated in a quartz cuvette at 254nm. The absorption spectra were recorded every 20 seconds until there was no significant change in absorption. As depicted in Figure 17, the irradiation at 254nm leads to the conversion of the *cis* isomer to the *trans* isomer. After irradiation of *cis* stilbene-4,4'-dicarboxylic acid at 254nm for 100 seconds, this solution (containing *cis* converted to *trans*) was irradiated in a pyrex tube at 350nm using a

350nm Rayonet lamp. The absorption spectra were recorded every 20 seconds. The 350nm irradiation converted the *trans* isomer back to the *cis* form (Figure 18). The *cis* stilbene-4,4'-dicarboxylic acid was also irradiated at 350nm and the absorption spectra were recorded every minute for 5 minutes. As shown in Figure 19 irradiation at 350nm did give slight change in the *cis* form. The *trans* stilbene-4,4'-dicarboxylic acid did not dissolve completely in ethanol and so it was filtered before use. This filtered solution was irradiated at 350nm in a pyrex tube. The absorption spectra were recorded every 20 seconds for 2 minutes. This irradiation as depicted in Figure 20 leads to the conversion of the *trans* isomer to the *cis*. After irradiation of *trans* stilbene-4,4'-dicarboxylic acid at 350nm for 2 minutes, this solution (containing *trans* converted to *cis*) was irradiated at 254nm. The absorption spectra were recorded every 20 seconds. The 254nm irradiation converts the *cis* isomer back to the *trans* form (Figure 21). The *trans* stilbene-4,4'-dicarboxylic acid was also irradiated at 254nm and the absorption spectra were recorded every minute for 5 minutes. As shown in Figure 22 irradiation at 254nm did not produce any significant change in the *trans* form.

**Figure 16.** Absorption spectra of *cis* stilbene-4,4'-dicarboxylic acid and *trans* stilbene-4,4'-dicarboxylic acid



The relative absorptions do not represent changes in extinction coefficients of the *cis* and *trans* compounds because the concentrations of *cis*-stilbene-4,4'-dicarboxylic acid and *trans*-stilbene-4,4'-dicarboxylic acid were different. The *cis* compound was soluble in ethanol and whereas the *trans* was not. The *trans* compound was soluble only in DMSO but DMSO was not used as the solvent for the UV-Vis studies as the UV cut-off of DMSO is quite high (268nm).

**Figure 17.** Absorption spectra of unirradiated *cis* stilbene-4,4'-dicarboxylic acid (0 sec) and irradiated *cis* stilbene-4,4'-dicarboxylic acid at 254nm.

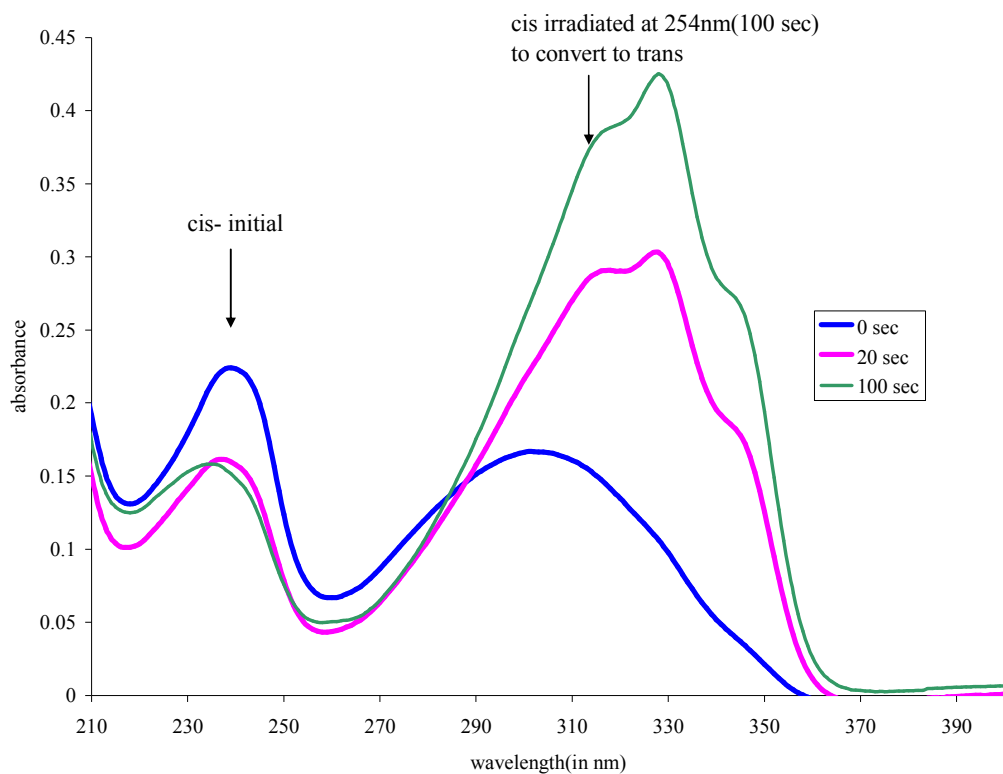
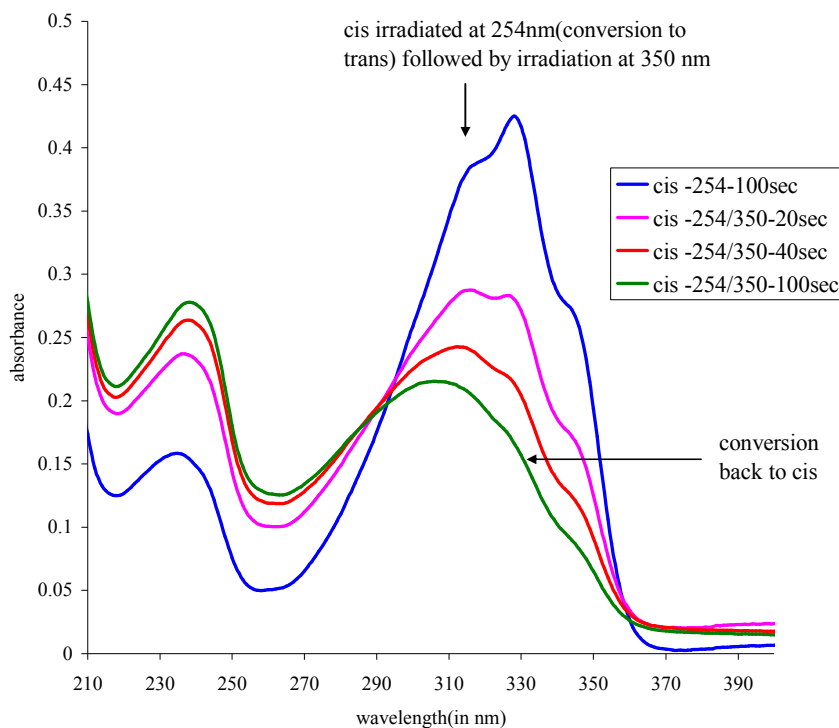
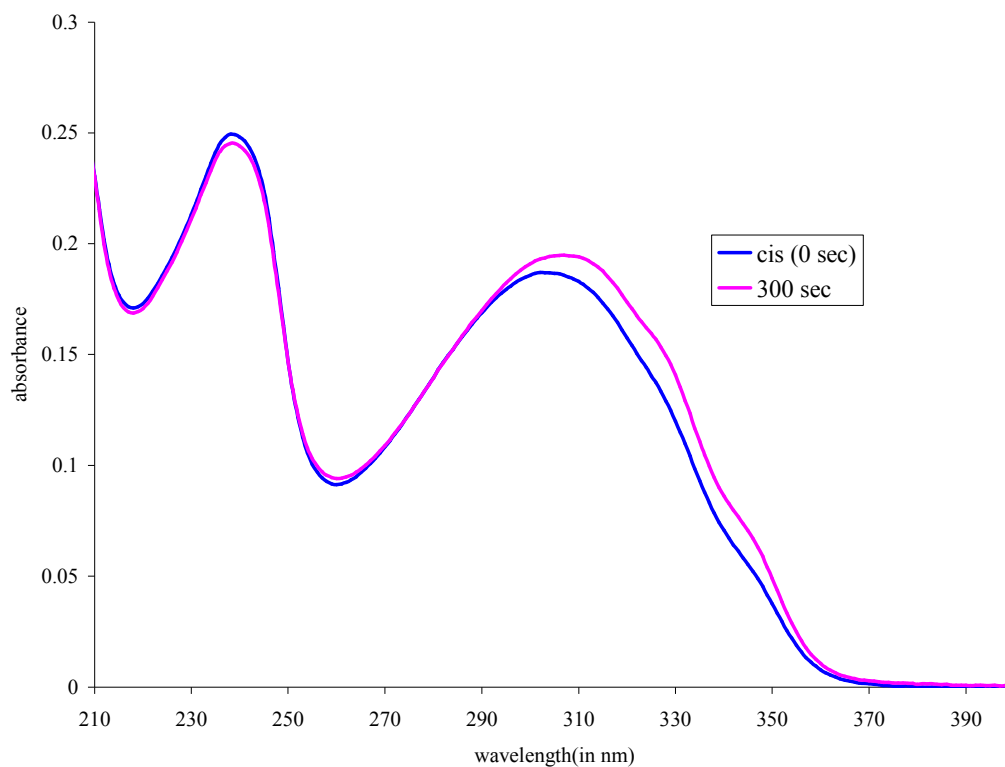


**Figure 18.** Absorption spectra of *cis* stilbene-4,4'-dicarboxylic acid irradiated at 254nm for 100 sec. (conversion to *trans*) and this solution irradiated again at 350nm.



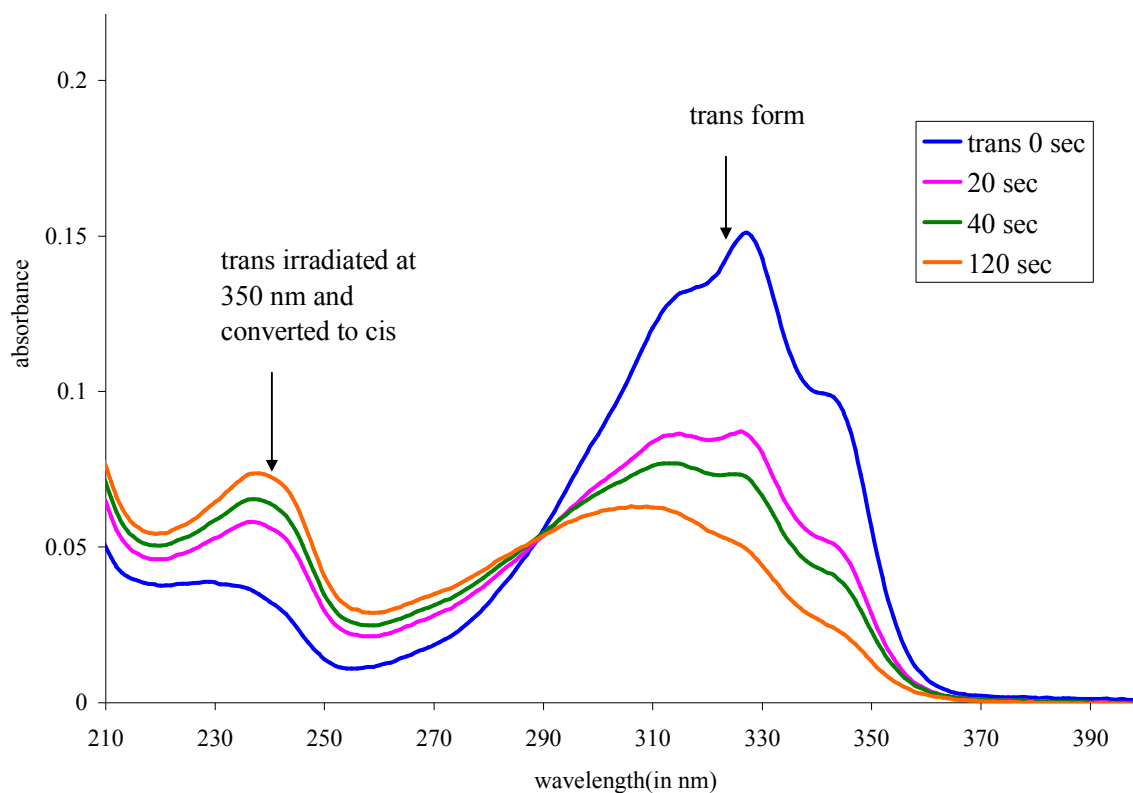
This spectrum shows the *cis* form irradiated at 254nm (100 sec) and converted to *trans* form and this solution irradiated at 350nm (100 sec) to convert back to *cis*. Comparison of the *cis* form generated after irradiation at 254nm → 350nm → 254nm and the original *cis* form suggests nearly complete conversion *cis* to *trans* and back to *cis*.

**Figure 19.** Absorption spectra of unirradiated *cis* stilbene-4,4'-dicarboxylic acid (0 sec) and irradiated *cis* stilbene-4,4'-dicarboxylic acid at 350nm.



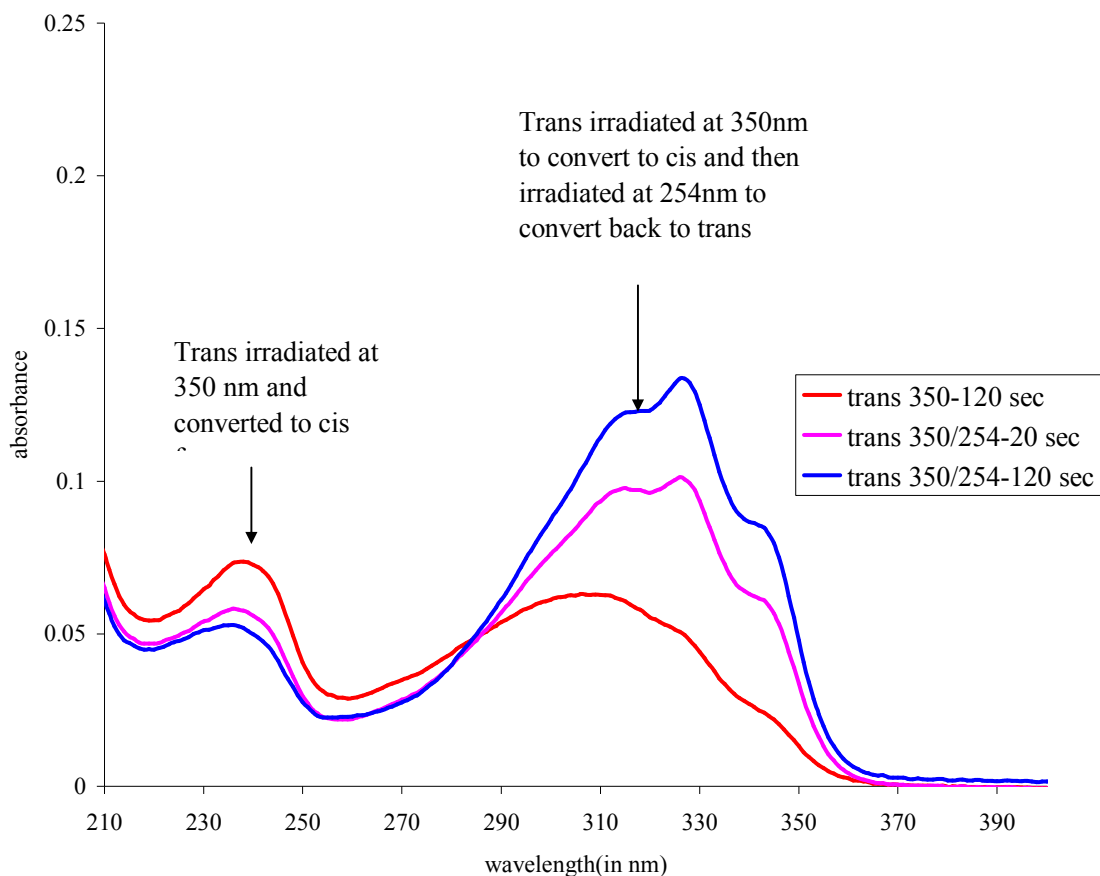
Irradiation of *cis* stilbene-4,4'-dicarboxylic acid was also carried at 350nm. This was done in order to determine the change in *cis* form compared to the change in *trans* form when they are irradiated at 350nm. After 300 second irradiation there was a very small bathochromic shift in the peak at 302nm.

**Figure 20.** Absorption spectra of unirradiated *trans* stilbene-4,4'-dicarboxylic acid (0 sec) and irradiated *trans* stilbene-4,4'-dicarboxylic acid at 350nm.



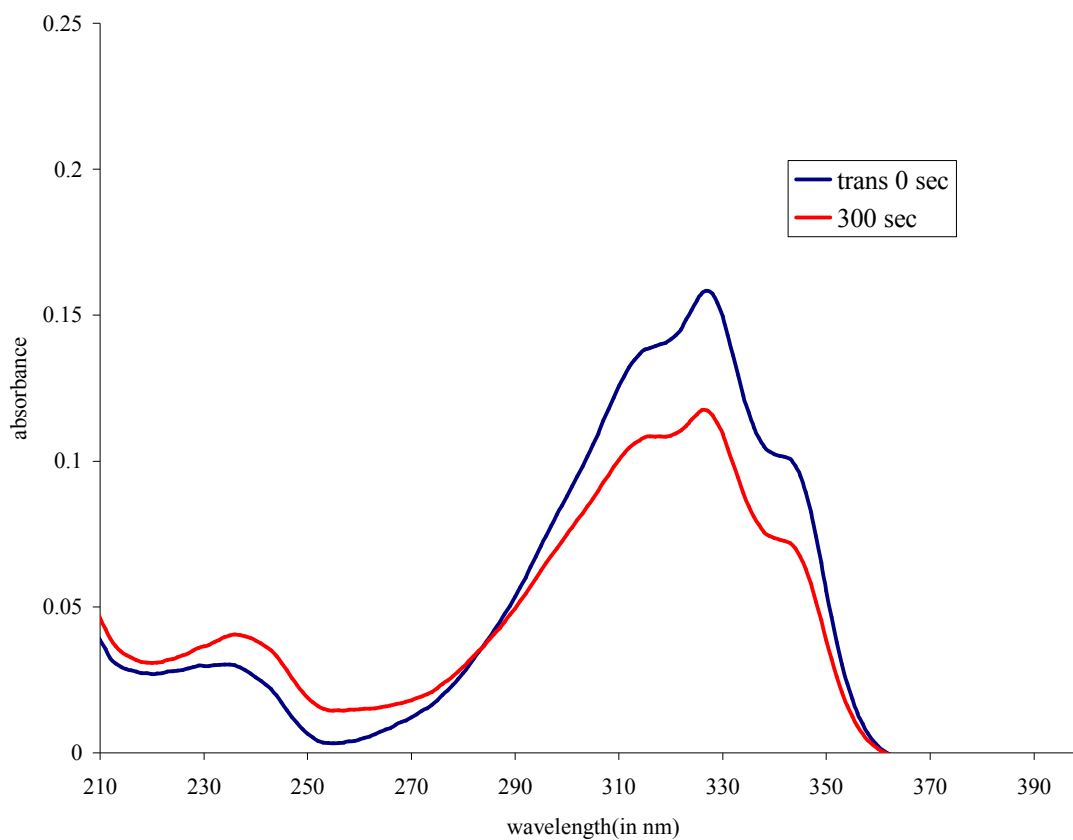
This spectrum shows the unirradiated *trans* form of stilbene-4,4'-dicarboxylic acid and the change in the *trans* form upon irradiation at 350nm. The peak at 317nm undergoes a hypsochromic shift indicating the isomerization to *cis* form.

**Figure 21.** Absorption spectra of *trans* stilbene-4,4'-dicarboxylic acid irradiated at 350nm for 120 sec. (conversion to *cis*) and this solution irradiated again at 254nm.



This spectrum shows the *trans* irradiated at 350nm(120 sec) and converted to *cis* form and this solution irradiated at 254 nm(120 sec) to convert back to the original *trans* form. Comparison of the *trans* form generated here and the original *trans* form shows that the absorbance at  $\lambda_{\max}$  is  $\sim 84\%$  of the original absorbance.

**Figure 22.** Absorption spectra of unirradiated *trans* stilbene-4,4'-dicarboxylic acid (0 sec) and irradiated *trans* stilbene-4,4'-dicarboxylic acid at 254nm.



Irradiation of *trans* stilbene-4,4'-dicarboxylic acid was also carried at 254nm. This was done in order to determine the change in *trans* compared to the change in *cis* when they are irradiated at 254nm. There is a decrease in the value of absorption of *trans* at its  $\lambda_{\max}$ (237nm). This indicates that when *trans* is irradiated at 254nm the isomerization to *cis* might be taking place.

The UV-Vis spectra suggests that irradiation of *cis*-stilbene-4,4'-dicarboxylic acid at 254nm converts it to the *trans* form and this *trans* form upon irradiation at 350nm can be converted back to the *cis* form. This conversion is almost complete. Irradiation of the *cis* form at 350nm results in a very small change in the absorption spectra. Irradiation of irradiation of *trans*-stilbene-4,4'-dicarboxylic acid at 350nm converts it to the *cis* form and this *cis* form upon irradiation at 254nm can be converted back to the *trans* form. Irradiation of the *trans* form at 254nm results in a some change in the absorption spectra which maybe due to the formation of the *cis* form.

<sup>1</sup>H- NMR spectra of *cis* and *trans* stilbene-4,4'-dicarboxylic acid and other subsequent compounds were recorded and may be found in Appendix A. <sup>1</sup>H- NMR (400 MHz, DMSO- *cis* stilbene-4,4'-dicarboxylic acid)  $\delta$  6.82(s, 2H), 7.31-7.33 (d, J=8.12Hz, 4H), 7.82-7.84(d, J=8.08Hz, 4H),12.8 (s,2H) .<sup>1</sup>H- NMR (400 MHz, DMSO- *trans* stilbene-4,4'-dicarboxylic acid)  $\delta$  7.49 (s, 2H), 7.75-7.77(d, J=8.17Hz, 4H), 7.94-7.96 (d, J=8.2Hz, 4H),13.07 (s,2H). NMR studies have shown that other than photoisomerization, in presence of certain solvents like benzene dimerization also occurs.<sup>(59)</sup> <sup>1</sup>H- NMR spectra of *cis* form(in DMSO) after irradiation at 254nm was also recorded. It shows the formation of *trans* isomer along with formation of dimer as indicated by the singlet at  $\delta$  4.72. <sup>1</sup>H- NMR spectra of *trans* form(in DMSO) after irradiation at 350nm was also recorded. It shows the formation of *cis* isomer along with dimer as indicated by the singlet at  $\delta$  4.66.

#### **4. Fabrication of film using 4-[(10-mercaptodecyl)pyridine-2,6-dicarboxylic acid as SAM**

The multilayer thin films III and IV (Figure 14- Section 1) were assembled using the non-covalent strategy described earlier. Each film consisted of the ligand stilbene-4,4'-dicarboxylic acid linked to the gold surface *via* metal-ligand interactions. These films were fabricated by self-assembly of 4-[(10-mercaptodecyl)pyridine-2,6-dicarboxylic acid on a clean gold surface, followed by the deposition of Cu(II) ions that complex with the head group of the SAM, and finally, deposition of the stilbene-4,4'-dicarboxylic acid ligand in either the *cis* (Film IV) or *trans* (Film III) form, which cap the Cu(II) ions. Characterization of these films was carried out using cyclic voltammetry, contact angle measurements and grazing incidence IR after the addition of each layer

Photoinduced isomerization of *cis* stilbene-4,4'-dicarboxylic acid capped film IV was attempted by irradiating the substrate in a quartz tube at 254nm with a Rayonet lamp. Photoinduced isomerization of *trans* stilbene-4,4'-dicarboxylic acid capped film III was attempted by irradiating the substrate with a 350nm Rayonet lamp in a pyrex tube. Characterization of the irradiated films was carried out using contact angle measurements and grazing incidence IR as described earlier.

Cyclic voltammograms of both III and IV (Figure 24) were obtained in an aqueous solution of potassium ferricyanide. The values of current generated changes as the individual components are deposited sequentially onto the gold surface. Gold is a conducting surface and so the CV of the bare gold surface shows the  $\text{Fe}^{3+}/\text{Fe}^{2+}$  redox

peaks for oxidation and reduction of ferricyanide.<sup>(42)</sup> When pyridine-capped decanethiol SAM is deposited the current is lowered ( $\sim 1\mu\text{A}$ ) indicating the formation of a well packed insulating layer. When the Cu(II) ions complex with the head group of the SAM the redox wave once again increases ( $\sim 120\mu\text{A}$ ) becoming almost similar to that of bare gold<sup>(21,22)</sup>. The increase in current could be due to the disorder created on the surface during deposition of the Cu(II) ions or could be because of the tunneling of electrons promoted by Cu(II) ions between the gold surface and the solution. Capping of the Cu(II) ions with the stilbene-4,4'-dicarboxylic acid ligand once again decreases the current indicating the formation of an insulating layer with some defects (Figure 23).

**Figure 23.** Cyclic voltammograms obtained for bare gold, pyridine decanethiol on gold (SAM), and Cu/pyridine decanethiol on gold (gold + SAM + Cu).

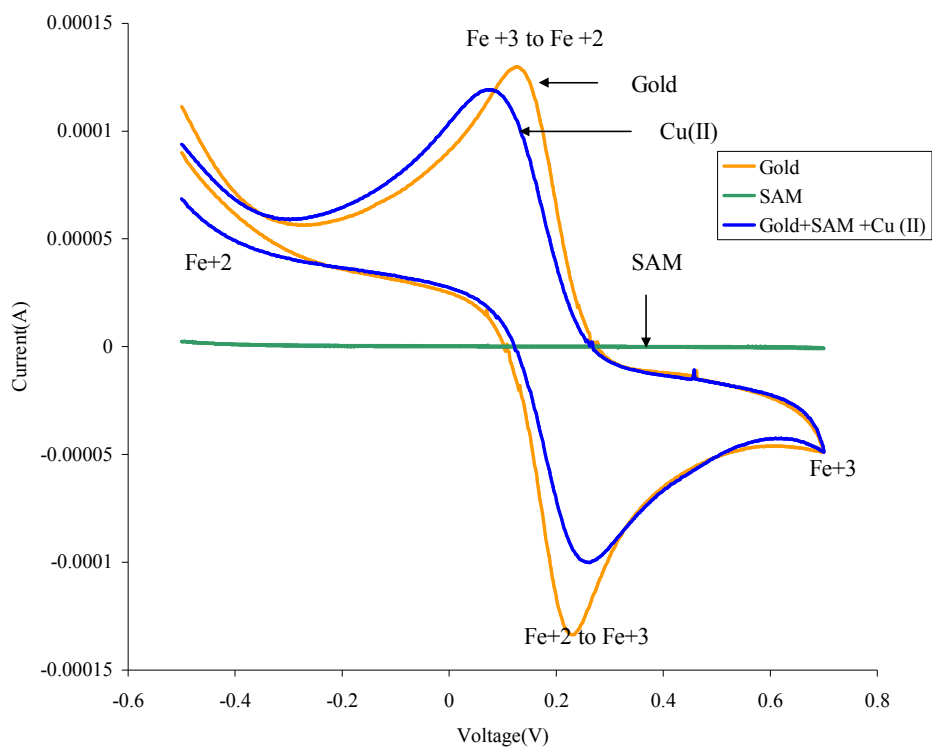
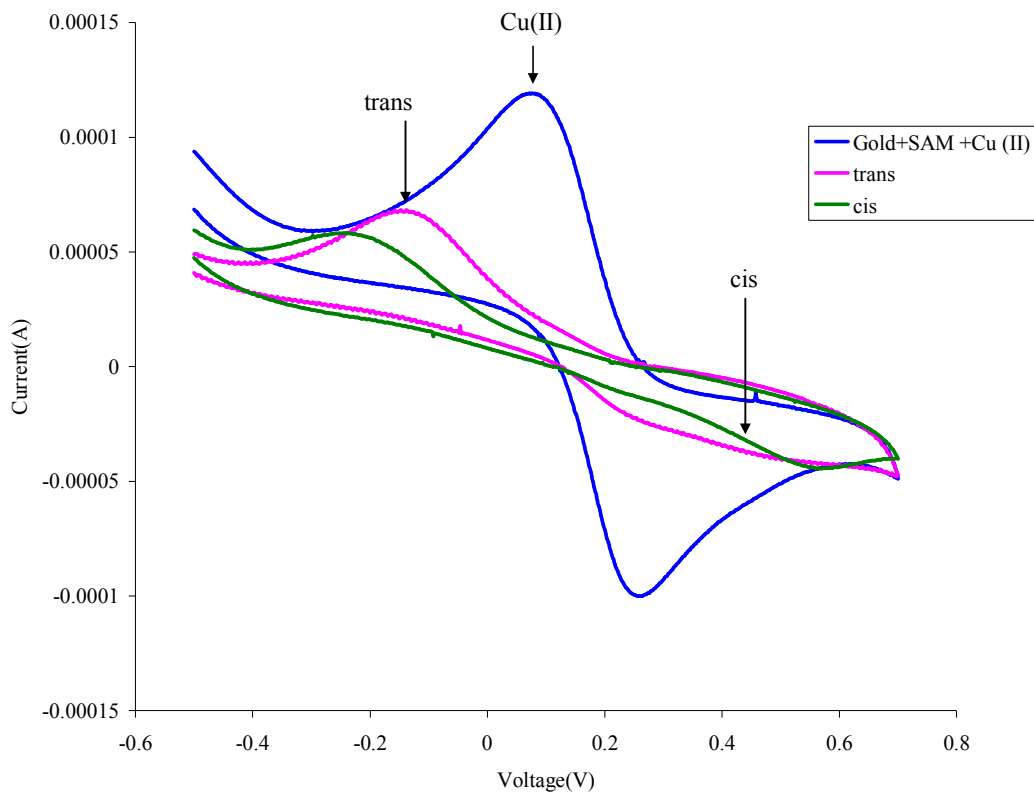


**Figure 24.** Cyclic Voltammograms of Cu/pyridine decanethiol on gold, Film III and Film IV



Contact angle measurements confirm the changes in the hydrophilicity of gold surface upon deposition of each layer. Contact angle measurements for the Film III and Film IV are given in Table 1. The Cu(II) ion surface (Figure 14, Film B) has a much smaller contact angle, differing from the dicarboxypyridyl capped surface (Figure 13, Film A) by  $\sim 15^\circ$ . This is possibly due to the ability of water to complex with Cu(II), which would make the surface considerably more hydrophilic, and hence decrease the contact angle.

Deposition of the *cis* stilbene-4,4'-dicarboxylic acid makes the surface hydrophobic while deposition of the *trans* stilbene-4,4'-dicarboxylic acid makes the surface hydrophilic as in the *trans* form the polar group –COOH is exposed to the surface. The contact angle values agreed with the assumptions that were made based on molecular modeling.

**Table 1.** Contact angle measurements for Films III and IV

Film	Contact angle (degrees)
Bare Gold	76 +/- 1.0
<b>Film IV</b>	
Component 1 (pyridyl-capped decanethiol)	74 +/- 2.0
Component 2 (Cu(II) ions)	52 +/- 2.0
Component 3 ( <i>cis</i> stilbene-4,4'-dicarboxylic acid )	76 +/- 2.5
<b>Film III</b>	
Component 1 (pyridyl-capped decanethiol)	74 +/- 2.0
Component 2 (Cu(II) ions)	52 +/- 2.0
Component 3 ( <i>trans</i> stilbene-4,4'-dicarboxylic acid )	50 +/- 2.0
Film IV irradiated at 254nm for 45 sec	65.5 +/- 2.5
Film IV irradiated at 254 nm for 60 sec	58 +/- 9.0

+/- 1.0 or +/- 2.0 etc. indicate the standard deviation.

IR measurements were carried out on film III and film IV as each layer was deposited. Moreover, IR spectra were collected after the films were irradiated. While the IR bands that distinguish between *cis*- and *trans*- stilbene-4,4'-dicarboxylic acids lie at frequencies lower than 1000 cm<sup>-1</sup>, the sensitivity of our grazing incidence IR instrument is low in this region. So the IR spectra were not used to differentiate between the Film III

and Film IV. The IR spectra were only used to verify the presence of each layer in the film.

**Table 2.** IR assignments for Film IV and irradiated Film IV. (The individual layers are: (i)pyridine decanethiol (ii) Cu<sup>2+</sup> (iii) *cis* stilbene-4,4'-dicarboxylic acid. (iv)Irradiated Film IV. The columns represent the peaks observed for the entire film following deposition of each component.)

The IR spectra are shown in Figures 25, 26, 27 and 28

Assignment	Peak frequency (cm <sup>-1</sup> )			
	Pyridine(Py)- decanethiol(dt)	Cu/Py-dt	<i>cis</i> stilbene-4,4'- dicarboxylic acid/Cu/Py-dt	Irradiated Film IV
v (CH arom)	3093	***	***	***
v <sub>a</sub> (CH <sub>2</sub> )	2921	2923	2929	2935
v <sub>s</sub> (CH <sub>2</sub> )	2852	2852	2854	2856
v (C=O)	1725	1725	1739	1739
	1691	1658	1679	1654
v (C-C aromatic)	1602	1606	1608	1612
Ar ring	1438	1428	1428	1425
	1392	1382	1392	1390
	1118	1122	1130	1122

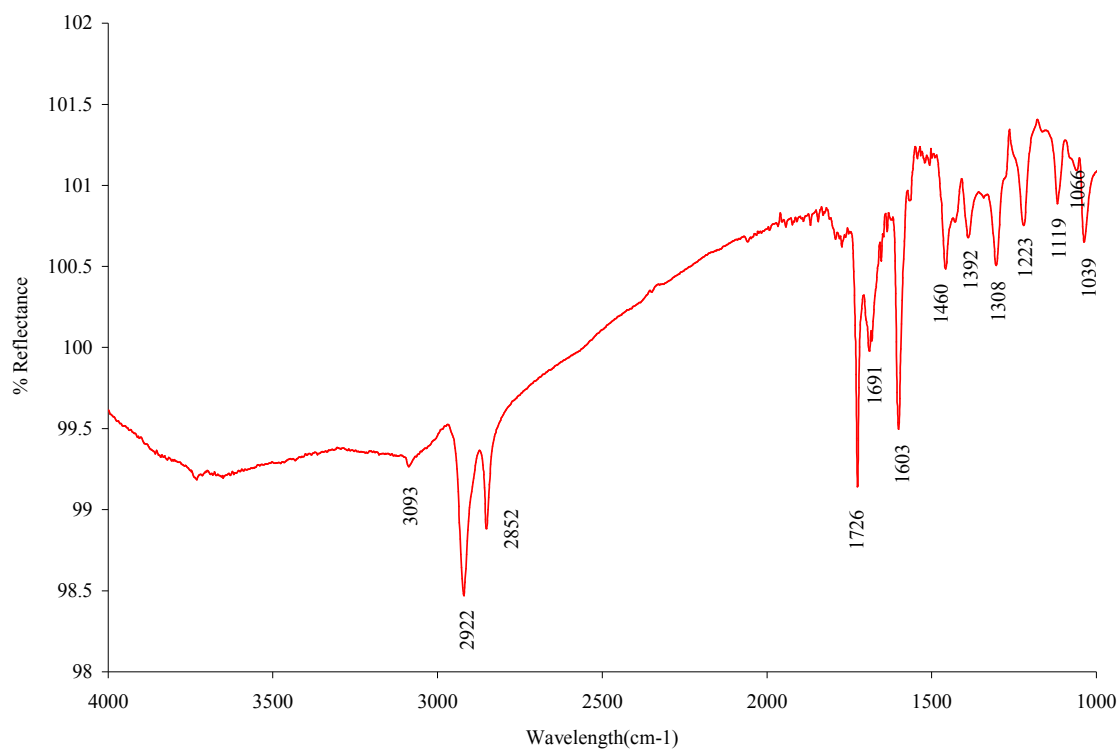
\*\*\*: not observed because of low intensity

**Table 3.** IR assignments for Film III and irradiated Film III. (The individual layers are: (i)pyridine decanethiol (ii) Cu<sup>2+</sup> (iii) *trans* stilbene-4,4'-dicarboxylic acid. (iv)Irradiated Film III. (The columns represent the peaks observed for the entire film following deposition of each component.)

The IR spectra are shown in Appendix A

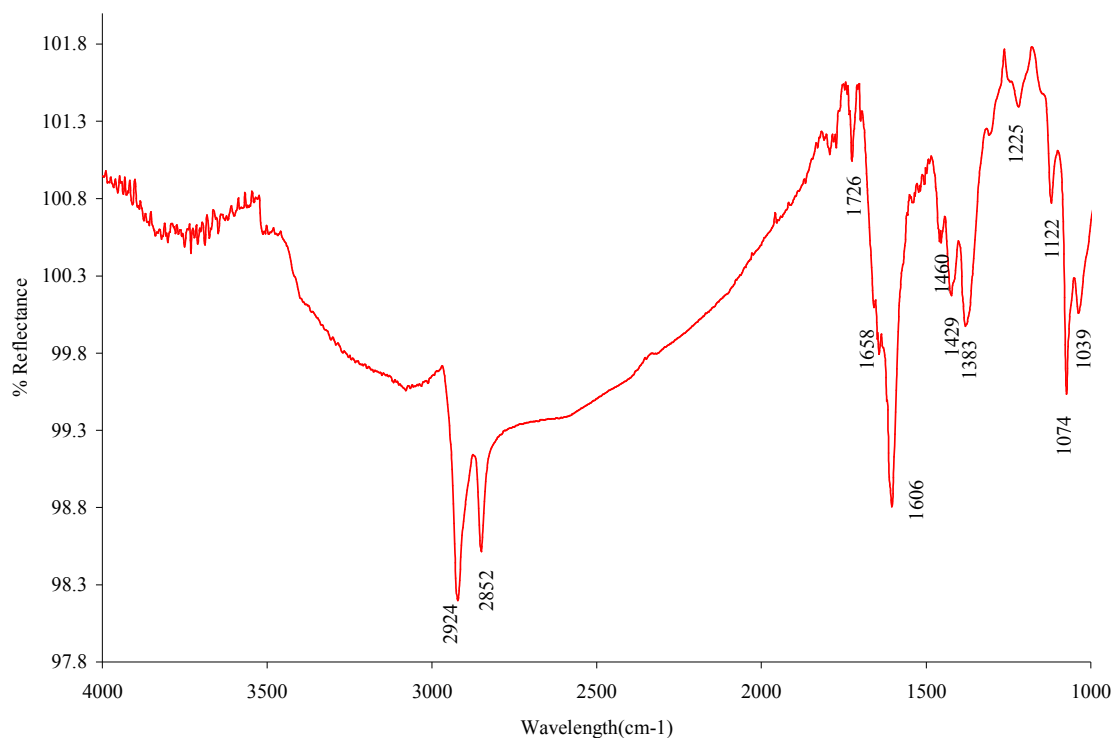
Assignment	Peak frequency (cm <sup>-1</sup> )			
	Pyridine(Py)- decanethiol(dt)	Cu/Py-dt	<i>trans</i> stilbene- 4,4'-dicarboxylic acid/Cu/Py-dt	Irradiated Film III
v (CH arom)	3093	***	***	***
v <sub>a</sub> (CH <sub>2</sub> )	2921	2923	2931	2937
v <sub>s</sub> (CH <sub>2</sub> )	2852	2852	2856	2852
v (C=O)	1725	1725	1737	1737
	1691	1658	1679	1662
v (C-C aromatic)	1602	1606	1606	1612
Ar ring	1438	1428	1425	1423
	1392	1382	1386	1388
	1118	1122	1120	1122

**Figure 25.** The grazing angle IR spectrum of a SAM of dicarboxypyridyl capped decanethiol.



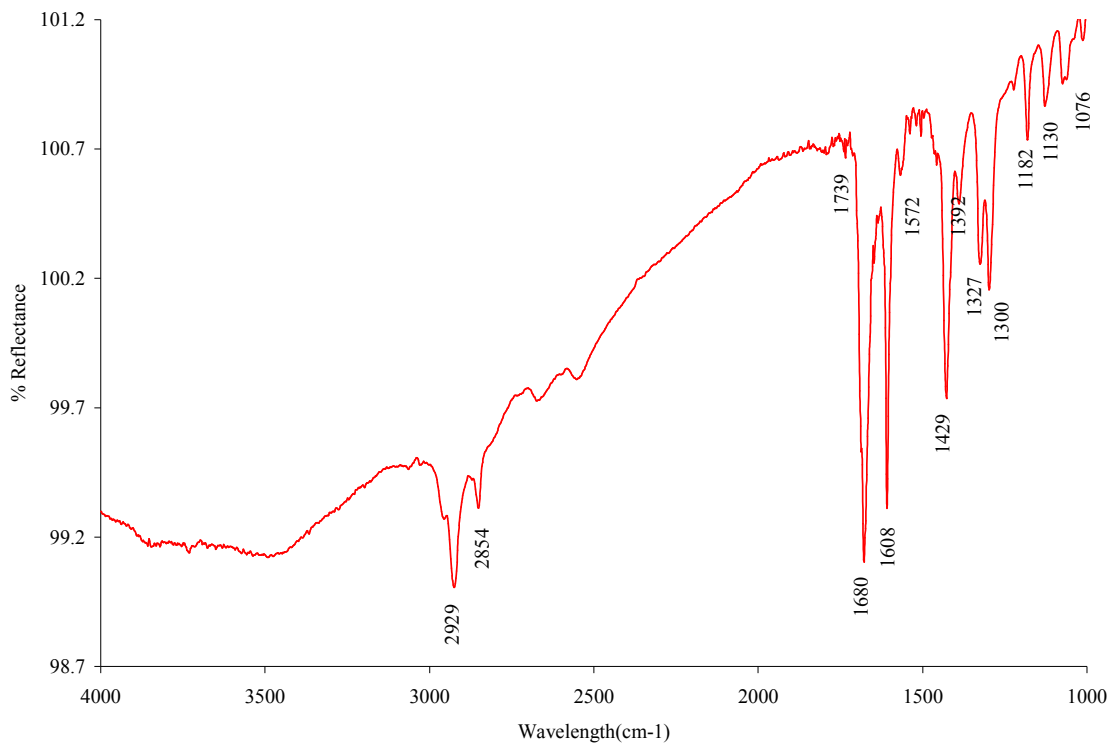
The presence of asymmetric stretching band of  $-\text{CH}_2$  at  $\sim 2921\text{cm}^{-1}$  indicates a well ordered and almost crystalline packing of the film.<sup>(9)</sup> The band at  $\sim 1725\text{cm}^{-1}$  and  $\sim 1691\text{ cm}^{-1}$  shows the presence of the  $-\text{C}=\text{O}$  group. This confirms the presence of SAM on the gold surface.

**Figure 26.** The grazing angle IR spectrum of dicarboxy pyridyl SAM complexed with Cu(II) ions.



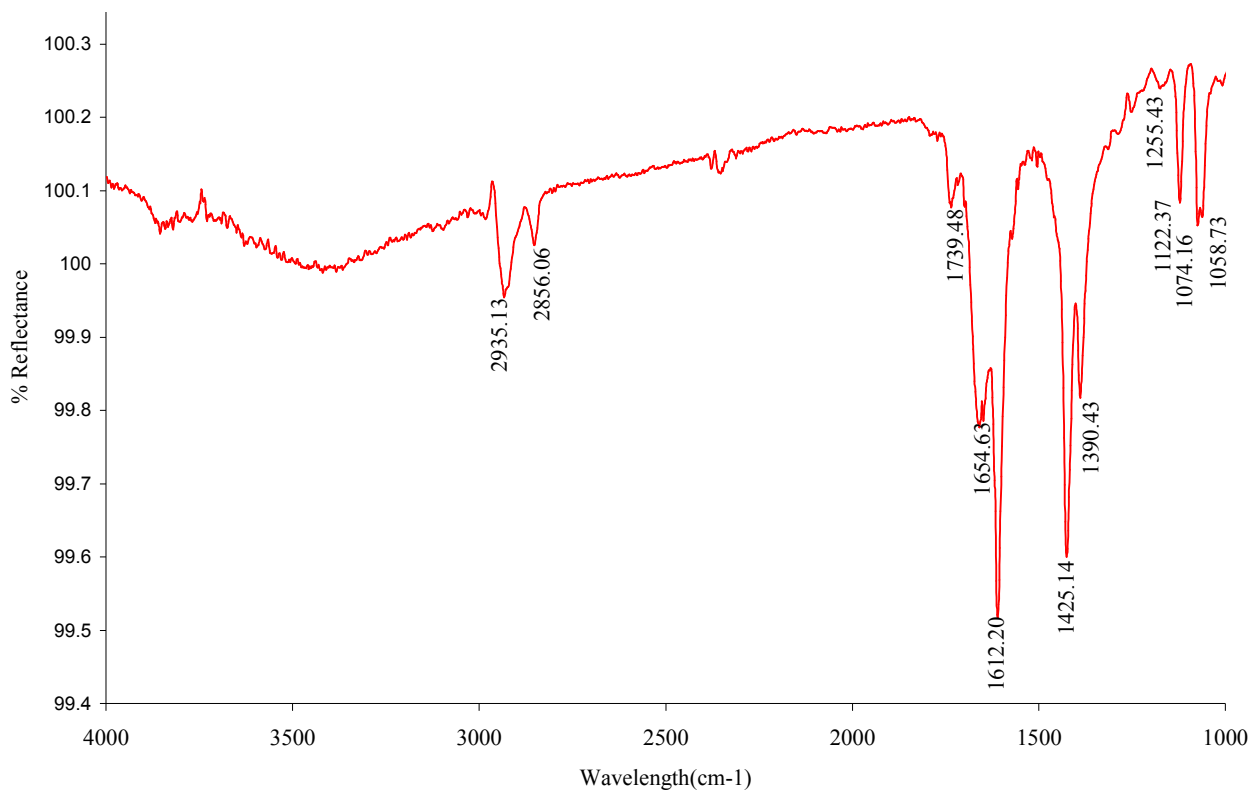
Complexation with Cu(II) brings about some disorder to the system as indicated by the increase in frequency of the  $\text{-CH}_2$  asymmetric stretching peak from  $\sim 2921\text{cm}^{-1}$  to  $\sim 2923\text{cm}^{-1}$ . There is a shift in the carbonyl peak to  $1658\text{cm}^{-1}$  indicating the formation of non-covalent bond between  $\text{-C=O}$  and Cu(II) .

**Figure 27.** The grazing angle IR spectrum of SAM + Cu(II) ions + *cis* stilbene-4,4'-dicarboxylic acid



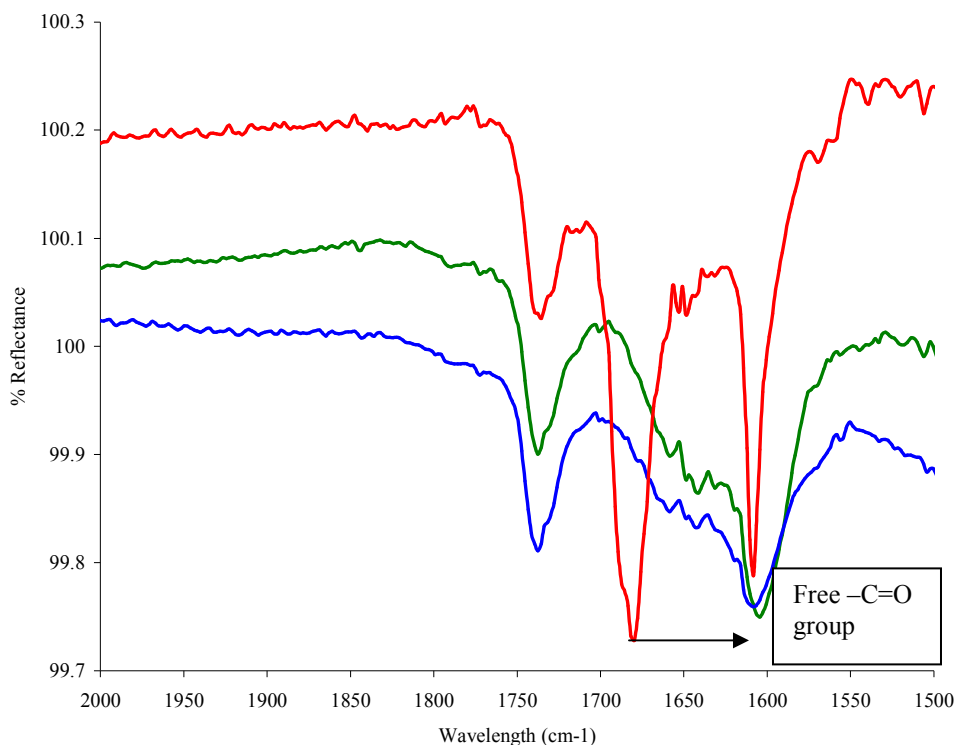
This IR spectrum resembles the IR spectrum on the solid *cis* stilbene-4,4'-dicarboxylic acid. This confirms the presence of *cis* stilbene-4,4'-dicarboxylic on the surface.

**Figure 28.** The grazing angle IR spectrum of Irradiated Film IV



The IR spectra of the irradiated Film IV resembles the IR spectra of structure B (Figure 14- SAM + Cu).

**Figure 29.** IR spectra of Films IV, irradiated IV and SAM+ Cu from 2000-1500  $\text{cm}^{-1}$



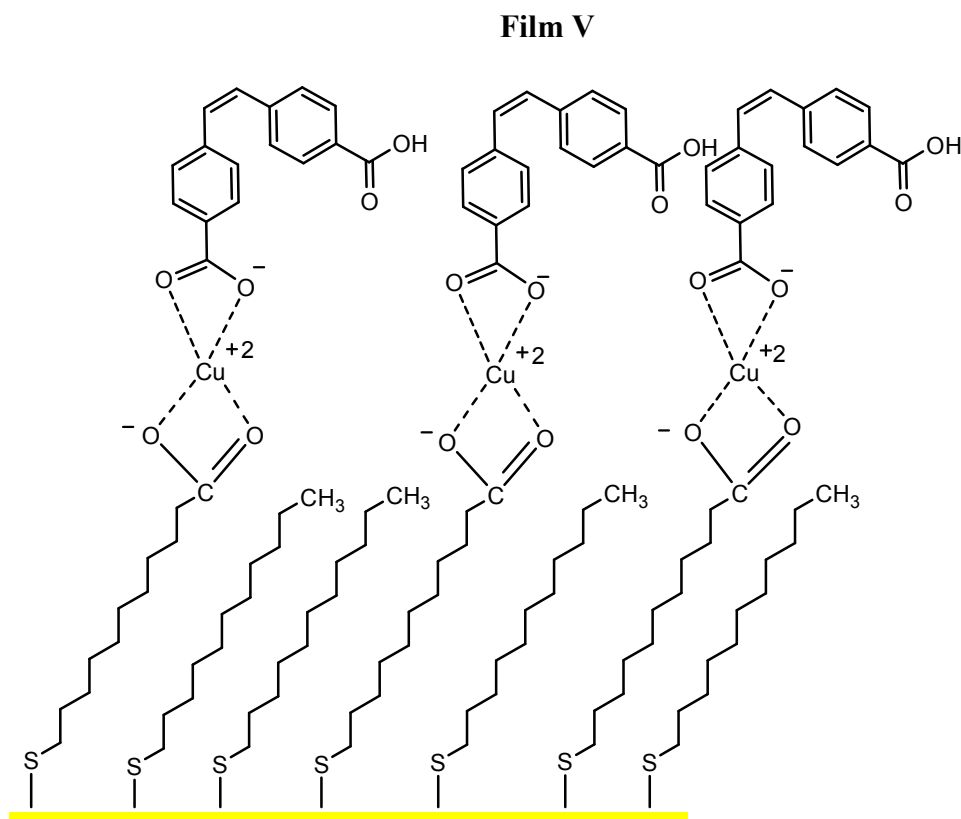
As shown in Figure 29 upon irradiation of Film IV at 254nm the IR band at  $\sim 1690\text{cm}^{-1}$  which corresponds to the free  $-\text{C}=\text{O}$  group of the *cis/trans* stilbene-4,4'-dicarboxylic acid disappears. IR of the irradiated Film IV (*cis* form) does not match with the IR of Film III but resembles to the film with SAM capped with Cu(II). This indicates that the film photodegrades.

As shown by the contact angle measurements, irradiation of Film IV (*cis* isomer) at 254nm for 45 seconds changes the contact angle by about  $10.5^\circ$  (Table 1). But the difference in the contact angle between the Film IV and Film III is more than  $25^\circ$ . Thus when the Film IV is irradiated at 254nm for about 45 seconds it does not convert

into the Film III. Further irradiation leads to a decrease of the contact angle to about  $\sim 58^\circ$  but the standard deviation of the contact angle measurements is very high ( $\sim 9^\circ$ ). The IR of the irradiated film IV indicates that when the film is irradiated for a sufficiently long time in order to bring about isomerization, the *cis* stilbene-4,4'-dicarboxylic acid layer is removed from the film. Thus *cis* to *trans* or *trans* to *cis* isomerization is blocked. Previous studies<sup>(60)</sup> carried out to bring about photoisomerization in SAMs indicate that in films that are well packed on the surface there is steric hindrance which prevents photoswitching. In films of azobenzene-derivatized alkanethiols, prolonged UV irradiation is known to lead to photodegradation of films and an associated reduction in water contact angles.<sup>(61)</sup>

## 5. Fabrication of film using mixed monolayers of mercaptoundecanoic acid and dodecanethiol

**Figure 30.** Fabrication of non-covalently assembled film using mixed SAMs



Multilayer films fabricated using 4-[(10-mercaptodecyl)pyridine-2,6-dicarboxylic acid as SAM (Figure 14-Section 1) did not facilitate the photoisomerization of stilbene-4,4'-dicarboxylic acid. Stearic hindrance generated from efficient packing of the film on the surface might have been the reason for prevention of photoswitching. To create space on the surface for depositing SAMs containing a photoisomerizable group Hu et al.<sup>(60)</sup> have used colloidal gold clusters instead of planar gold surfaces. The packing on gold cluster is not as ordered as the packing on a planar gold surface. Thus in a gold cluster there is enough space for the SAM to undergo photoisomerization. Mixed or two

component monolayers have also been used to create space on the surface.<sup>(61)</sup> Mixed monolayers on gold surface have been studied for many years.<sup>(13,62-67)</sup> Mixed monolayers formed from functionalized alkanethiols having head groups –Br,-OH,-COOH and alkanethiols with –CH<sub>3</sub> head group distribute uniformly in the SAM surface without aggregating into domains of more than a few tens of angstroms across.<sup>(13)</sup> i.e. they do not phase separate macroscopically. Thus for a surface comprising of a two-component SAM the overall properties of the surface will arise from the contribution of both the components of the mixed monolayer. We used the mixed monolayers for creating space for our non-covalently assembled monolayers (Figure 30). For a mixed monolayers comprising of mercaptoundecanoic acid and dodecanethiol, the mercaptoundecanoic acid can be used to fabricate a non-covalently linked multilayer. The head group (-CH<sub>3</sub>) of dodecanethiol will not bind to the copper ions in our multilayer system and thus act as a spacer unit.

Mixed SAMs derived from ethanolic solutions of different concentrations of mercaptoundecanoic acid and dodecanethiol (total thiol concentration = 1mM) were characterized using X-ray Photoelectron Spectroscopy (XPS).<sup>(13)</sup> The XPS data showed that when the mole fraction of mercaptoundecanoic acid in solution was 0.7 then the mole fraction of mercaptoundecanoic acid on the surface was ~0.5. Mole fraction of the acid on the surface was calculated from the intensity of photoelectron of oxygen(1s) generated from XPS data. Based on this study a solution containing 0.7mM mercaptoundecanoic acid and 0.3mM dodecanethiol was used for our non-covalently assembled multilayer systems (Film V). Characterization of Film V was carried out by

cyclic voltammetry, IR and contact angle. The IR of the irradiated Film V does not resemble the IR of the film containing the *trans* stilbene-4,4'-dicarboxylic acid but resembles the IR of the mixed monolayer + Cu (Figure 31). Thus, this two-component system does not facilitate the *cis-trans* isomerization.

**Table 4.** Contact angle measurements(Film V)

Film	Contact angle (degrees)
Bare Gold	76 +/- 1.0
Film V	
Component 1(mixed monolayer: 0.7mM mercaptoundecanoic acid + 0.3 mM dodecanethiol)	55 +/- 2.0
Component 2 (Cu(II) ions)	50 +/- 2.0
Component 3 ( <i>cis</i> stilbene-4,4'-dicarboxylic acid )	70 +/- 2.0
Film V irradiated at 254nm for 45 sec	60 +/- 2.5

The cyclic voltammograms of bare gold, mixed monolayer (0.7mM mercaptoundecanoic acid and 0.3 mM dodecanethiol) on gold, Cu/mixed monolayer on gold and *cis* stilbene-4,4'-dicarboxylic acid on Cu(II) are given in Appendix A. As described earlier the current decreases on formation of SAM, increases on deposition of Cu(II) ions and once again decreases on deposition of *cis* stilbene-4,4'-dicarboxylic acid.

**Figure 31.** IR spectra of irradiated Film V and mixed monolayer + Cu(II)+ *trans* from  $2000\text{cm}^{-1}$  to  $1000\text{cm}^{-1}$

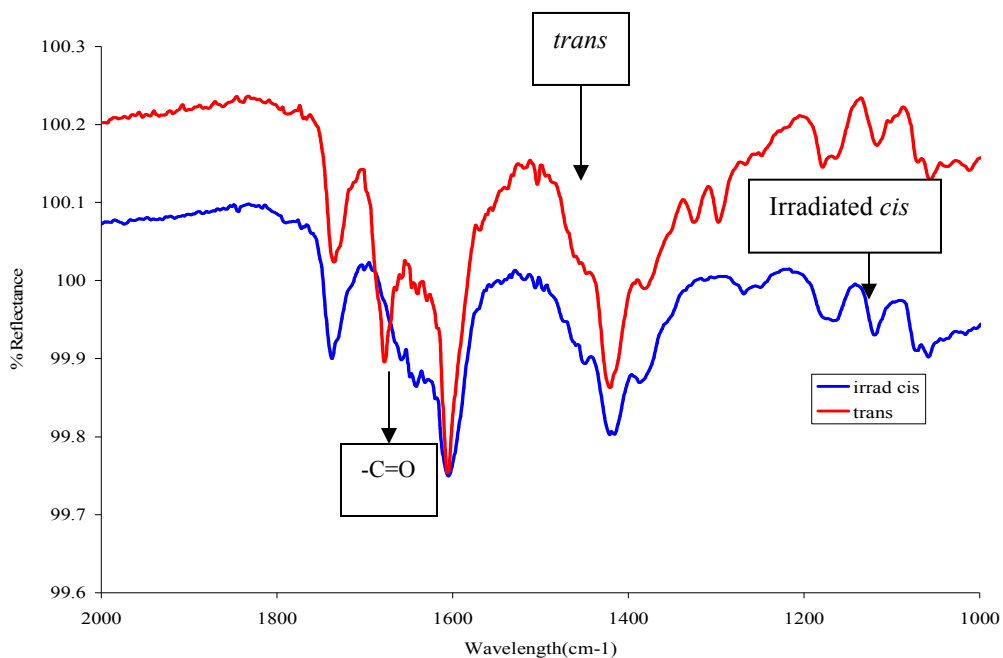
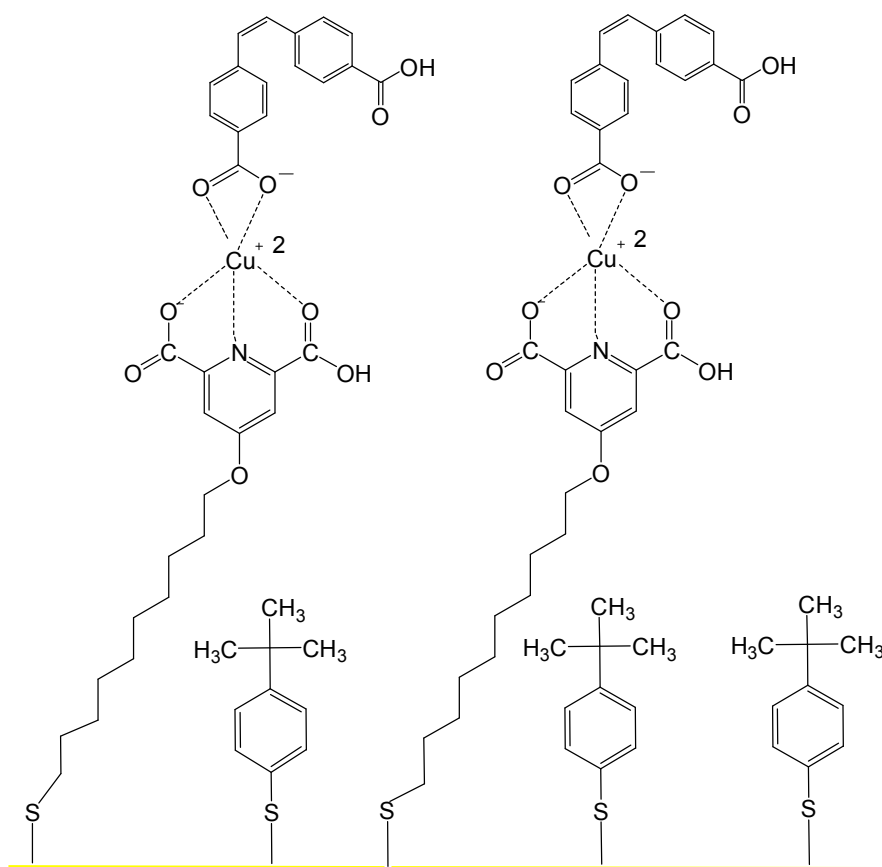


Figure 31 shows that the IR spectrum of irradiated Film V does not match the IR spectra of *trans* form. The peak at  $1690\text{cm}^{-1}$  which corresponds to the free  $\text{-C=O}$  is present in the IR spectra of Film V. As shown in the figure this peak is not seen in the spectra of the irradiated Film V indicating the degradation of the film. Thus, mixed monolayers of mercaptoundecanoic acid and dodecanethiol do not facilitate photoisomerization.

6. **Fabrication of film using mixed monolayers of 0.5mM 4-[(10-mercaptodecyl)pyridine-2,6-dicarboxylic acid and 0.5mM 4-tert-butylbenzenethiol**

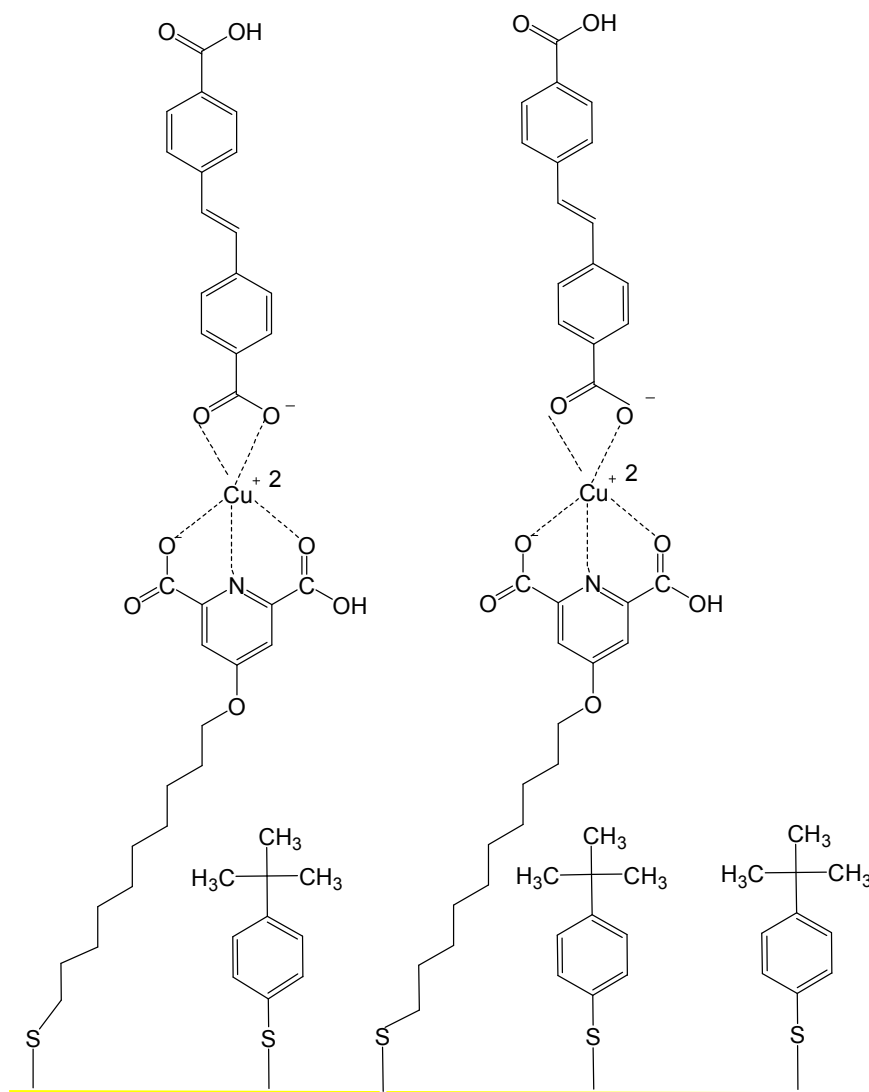
**Figure 32.** Fabrication of non-covalently assembled film using mixed SAMs (using *cis* form of stilbenes-4,4'-dicarboxylic acid)

**Film VII**



**Figure 33.** Fabrication of non-covalently assembled film using mixed SAMs (using *trans* form of stilbenes-4,4'-dicarboxylic acid)

**Film VIII**

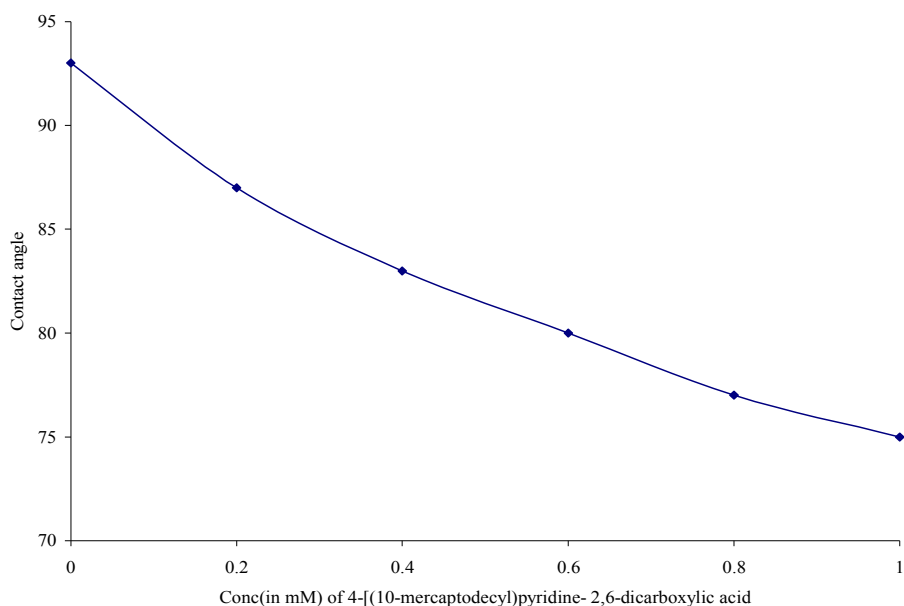


To facilitate the *cis-trans* photoisomerization on the surface, more space was created on the surface using mixed monolayers of 4-[(10-mercaptodecyl)pyridine-2,6-dicarboxylic acid and 4-*tert* butylbenzenethiol. Film VII was fabricated using non-covalent linkage (Figure 32). This film was characterized using cyclic voltammetry, IR, ellipsometry and contact angle. Irradiation of the film was carried out at 254nm and later

at 350nm. A similar film was fabricated by using *trans* stilbene-4,4'-dicarboxylic acid as ligand (Figure 33). This film (Film VIII) was also characterized using cyclic voltammetry, IR, contact angle and ellipsometry. This film was first irradiated at 350nm and later irradiated at 254nm.

The contact angles of SAMs derived from ethanolic solutions containing different concentrations of mixed monolayers of 4-[(10-mercaptodecyl)pyridine-2,6-dicarboxylic acid and 4-tert butylbenzenethiol (total thiol concentration is 1mM) were recorded. The graph of Contact Angle vs Concentration of 4-[(10-mercaptodecyl)pyridine-2,6-dicarboxylic acid (Figure 34) indicates the presence of both 4-[(10-mercaptodecyl)pyridine-2,6-dicarboxylic acid and 4-tert butylbenzenethiol on the surface.

**Figure 34.** Variation in the values of contact angle as a function of the concentration of 4-[(10-mercaptodecyl)pyridine-2,6- dicarboxylic acid in solution.



Ellipsometric measurements were carried out after the deposition of each layer from Film VII and Film VIII. The values (as range) are given in Table 5. As shown by the data upon deposition of each layer there is an increase in the thickness of the film.

**Table 5.** Ellipsometric data for Film VII and Film VIII

Film	Thickness in nm
Mixed Monolayer	1.0-1.2
Mixed Monolayer with Cu(II)	1.0-1.3
Film VII	1.6-1.8
Film VIII	1.6-1.9

As shown in Figure 35 cyclic voltammetry was used to follow the deposition of each layer. As the Figure 35 shows, the capping of Cu(II) with *cis* stilbene-4,4'-dicarboxylic acid forms an insulating layer with some defects. The Figure 36 indicates that the *trans* stilbene-4,4'-dicarboxylic acid does not form a very well insulating layer. Figure 37 gives a comparison of the CV of Film VII and irradiated Film VII.

**Figure 35.** Cyclic voltammograms obtained for bare gold, mixed monolayer on gold and Cu/mixed monolayer on gold, *cis* stilbene-4,4'-dicarboxylic acid on Cu

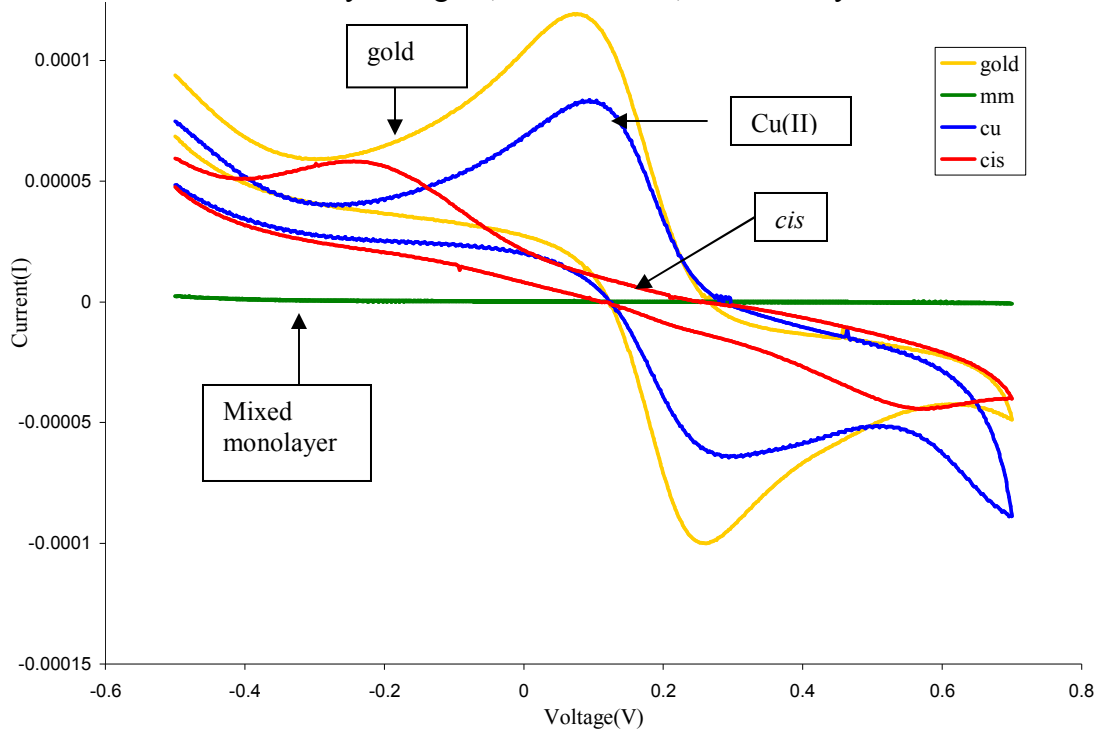


**Figure 36.** Cyclic voltammograms obtained for bare gold, mixed monolayer on gold and Cu/mixed monolayer on gold, *trans* stilbene-4,4'-dicarboxylic acid on Cu

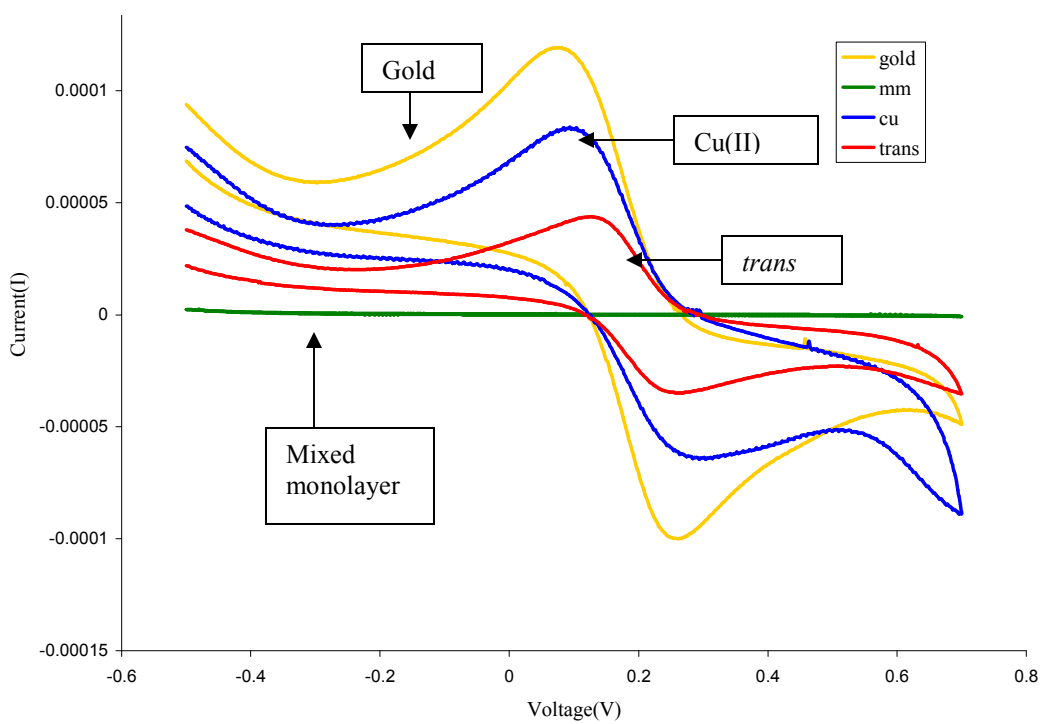
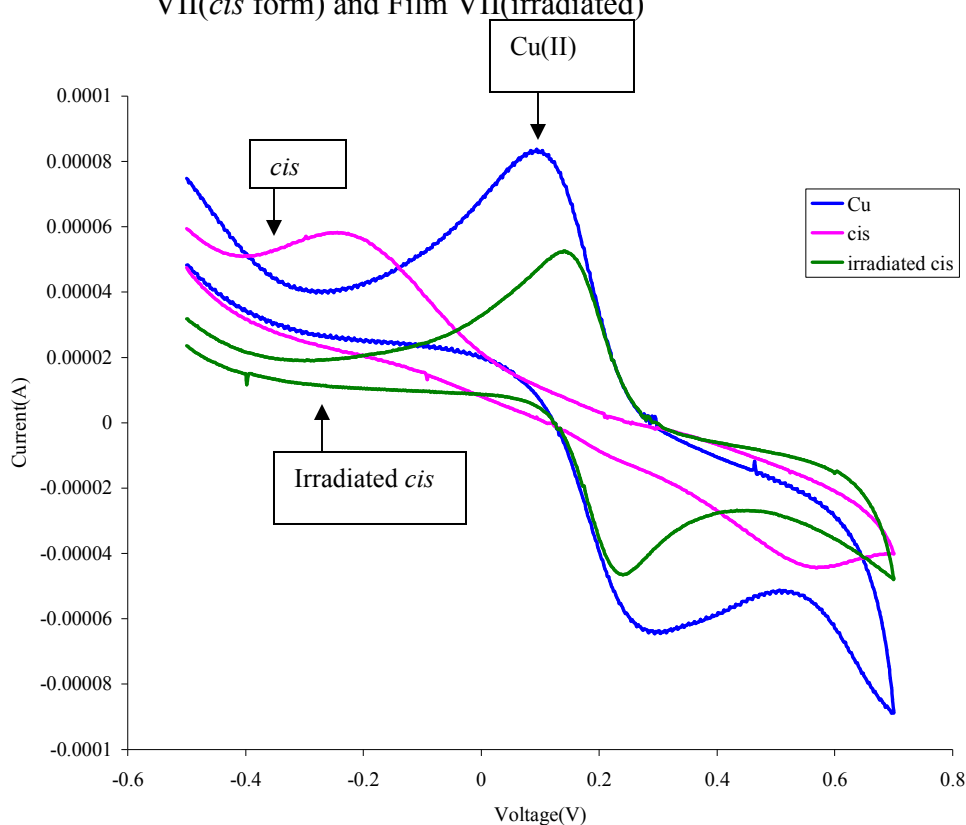


**Figure 37.** Cyclic voltammograms obtained for mixed monolayers + Cu(II) and Film VII(*cis* form) and Film VII(irradiated)



The deposition of each layer of Film VII and Film VIII is followed by contact angle measurements. Moreover, the contact angle measurements are recorded after the irradiation of Film VII at 254nm (conversion to *trans* form), followed by irradiation at 350nm (conversion back to the *cis* form) (Table 6). The contact angles are also recorded after the irradiation of Film VIII at 350nm (conversion to the *cis* form), followed by irradiation at 254 nm (conversion back to the *trans* form) (Table 7). As Table 7 shows that irradiation of Film VII at 254nm converts the *cis* form to the *trans* form leading to a decrease in contact angle of  $\sim 25^\circ$ . The decrease in contact angle of  $\sim 25^\circ$  is much greater than that reported for a variety of photo-isomerizable thin films of azobenzenes or

spiropyrans that typically exhibit changes of  $\sim 9^\circ$ .<sup>(68)</sup> Moreover, irradiation of Film VII at 254nm followed by irradiation at 350 nm increases the contact angle by  $\sim 21^\circ$ . These changes show the photoswitching of the Film VII. As Table 7 indicates, the Film VIII also exhibits reversible photoswitchable wettability. The Film VII was completely reversible for one cycle i.e. *cis* was converted to *trans* and back to *cis*. When the Film VII was irradiated at 254nm followed by 350nm and then by 254nm(second cycle) the contact angle (Table 6) did not change significantly. The value of the contact angle generated upon irradiation at 254nm following the first cycle is close to the contact angle value of Film VII instead of Film VIII. As the UV-Vis spectra of the films on the surface could not be obtained the changes occurring on the surface cannot be explained. One assumption made is that the stilbene moiety reaches a photostationary state in the second cycle of irradiation which prevents further change in wettability. The Film VII photodegrades upon prolonged irradiation (40 minutes) at 254nm. The photodegradation is indicated by the increase in contact angle to  $\sim 80^\circ$  which corresponds to the contact angle of the mixed SAM. Moreover the IR spectra after irradiation (second cycle) resembles the IR spectra of the mixed SAM.

**Table 6.** Contact angle measurements following the deposition of each layer of Film VII and after irradiation of Film VII

Film	Contact angle (degrees)
Bare Gold	76 +/- 1.0
<b>Film VII</b>	
Component 1 (mixed monolayer: 0.5mM 4-[(10-mercaptodecyl)pyridine-2,6-dicarboxylic acid + 0.5 mM 4- <i>tert</i> butylbenzenethiol)	80 +/- 2.0
Component 2 (Cu(II) ions)	55 +/- 2.0
Component 3 ( <i>cis</i> stilbene-4,4'-dicarboxylic acid )	70 +/- 2.0
Film VII irradiated at 254nm (5 min)	45 +/- 2.0
Film VII irradiated at 350nm (after being irradiated at 254nm)(30 min)	66 +/- 1.0
Film VII irradiated at 254nm (after being irradiated at 254nm and 350 nm)(5 min)	62 +/- 2.0

**Table 7.** Contact angle measurements following the deposition of each layer of Film VIII and after irradiation of Film VIII

Film	Contact angle (degrees)
Bare Gold	76 +/- 1.0
<b>Film VIII</b>	
Component 1 (mixed monolayer: 0.5mM 4-[(10-mercaptodecyl)pyridine-2,6-dicarboxylic acid + 0.5 mM 4- <i>tert</i> butylbenzenethiol)	80 +/- 2.0
Component 2 (Cu(II) ions)	55 +/- 2.0
Component 3 ( <i>trans</i> stilbene-4,4'-dicarboxylic acid )	45 +/- 2.0
Film VIII irradiated at 350nm	65 +/- 2.5
Film VIII irradiated at 254nm (after being irradiated at 350nm)	48 +/- 2.0

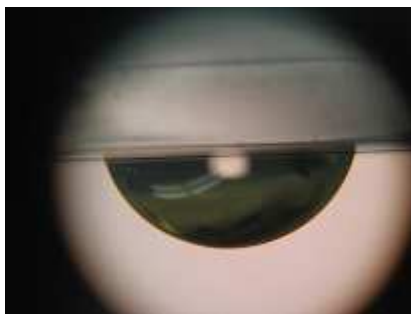
**Figure 38.** Contact Angle Photos.



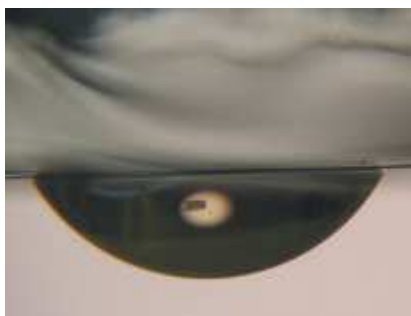
Contact angle of water on mixed SAM of 4-[(10-mercaptodecyl)pyridine-2,6-dicarboxylic acid and 4-*tert* butylbenzenethiol, indicating a hydrophobic surface



Contact angle of water on Cu(II) capped mixed SAMs, formation of a hydrophilic surface as indicated by decrease in the contact angle



Contact angle of water on Film VI  
Formation of hydrophobic surface



Contact angle of water on Film VI after irradiation at 254 nm. Formation of Film VII i.e. the *trans* form and thus the surface becomes hydrophilic

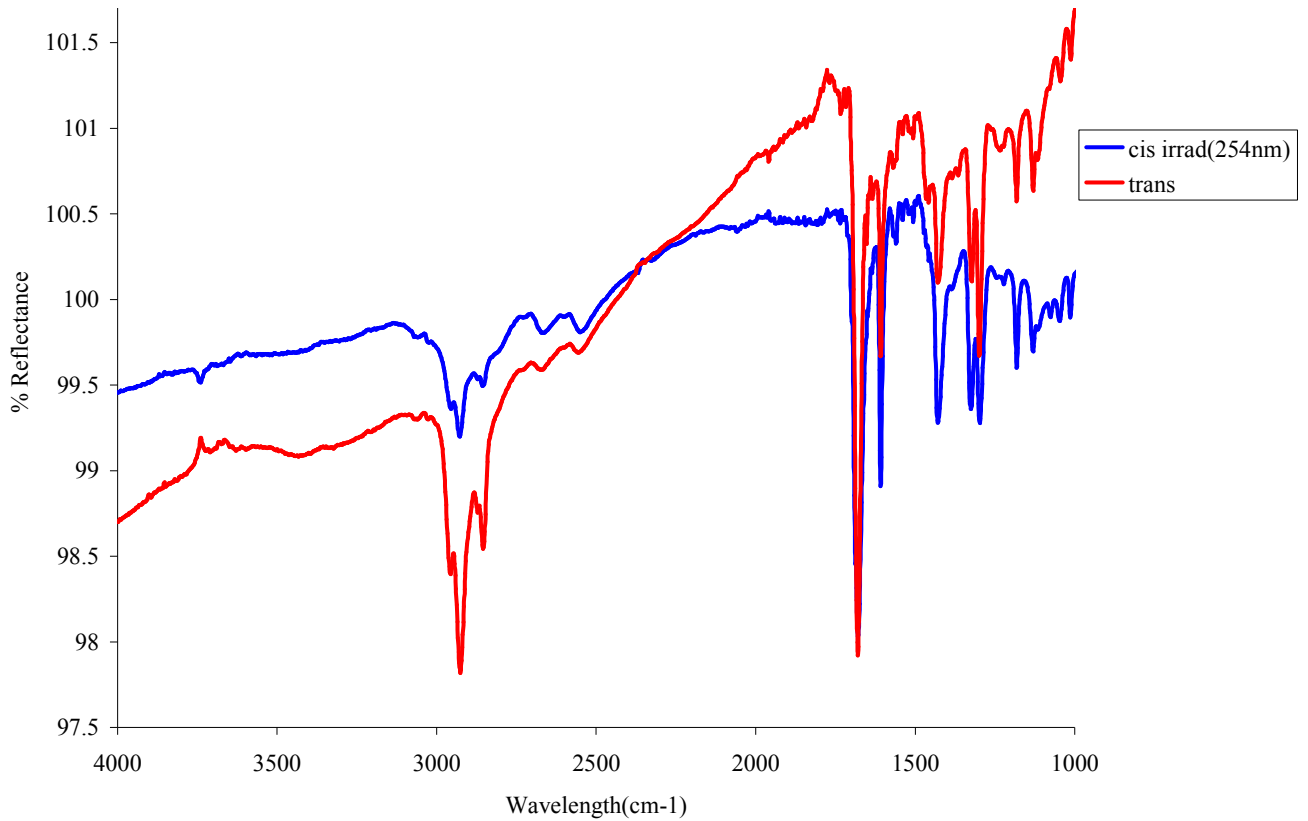


Contact angle of water on Film VI after irradiation at 254nm followed by irradiation at 350nm. Surface becomes hydrophobic due to formation of *cis* form

IR spectra were collected after deposition of each layer for Film VII and Film VIII. As discussed earlier the IR absorption bands that distinguish between *cis*- and *trans*-stilbene-4,4'-dicarboxylic acids lie at frequencies lower than  $1000\text{ cm}^{-1}$ , the sensitivity of our grazing incidence IR instrument is low in this region. The IR spectra were also collected after the irradiation of the both films. These spectra were used to confirm the presence of the stilbene moiety and to prove that for the first irradiation cycle the film is

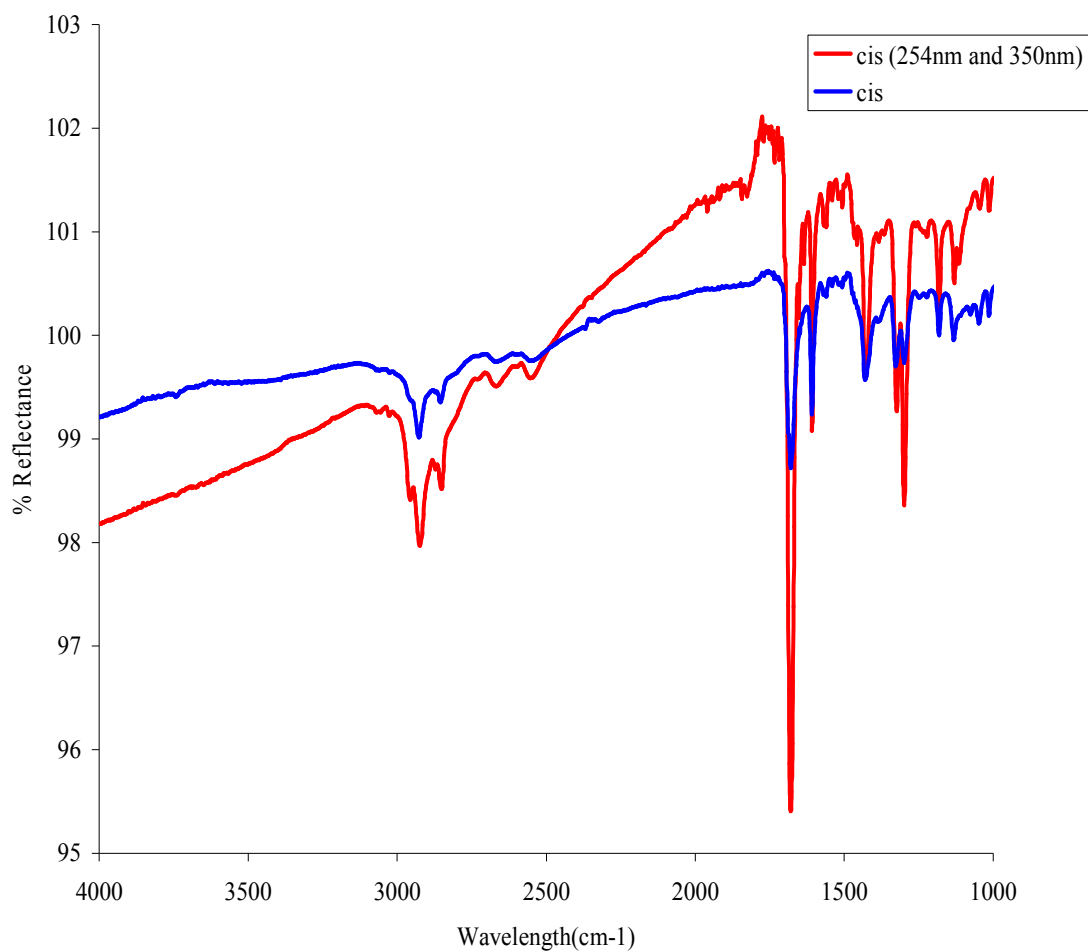
intact. As the Figures 39 and 40 indicate, the irradiation of the films at 254nm/350nm (first cycle only) does not destroy the films.

**Figure 39.** IR spectra of irradiated Film VII (at 254nm) and Film VIII



The above figure contains spectra of Film VII irradiated at 254nm and Film VIII. This spectra shows that irradiation (254nm, first cycle) does not lead to photodegradation of the film.

**Figure 40.** IR spectra of irradiated Film VII (at 254nm followed by irradiation at 350nm) and Film VII



The above spectra show that irradiation of *cis* at 254nm and later at 350nm (first cycle only) does not photodegrade the film.

## Conclusion

Multilayer films of 4-[(10-mercaptodecyl)oxy]pyridine-2,6-dicarboxylic acid + Cu(II)+ *cis/trans* stilbene-4,4'-dicarboxylic acid were fabricated. Irradiation of these films did not result in photoisomerization of the stilbene moiety. It is believed that photoisomerization was prevented because of steric hindrance arising from well packed films. To facilitate photoisomerization, space was created on the surface by using mixed monolayers. Multilayer films were fabricated with mixed monolayers of mercaptoundecanoic acid and dodecanethiol as SAMs. The Cu(II) ions do not bind to the dodecanethiol creating in space on the surface. The irradiation of these films also did not facilitate isomerization of the stilbene-4,4'-dicarboxylic acid. When 4-[(10-mercaptodecyl)oxy]pyridine-2,6-dicarboxylic acid and 4-*tert* butylbenzenethiol were used as mixed SAMs enough space was created on the surface to photoisomerize stilbene-4,4'-dicarboxylic acid and control the wettability of the surface. The contact angle and IR data suggests that the photoisomerization was complete for one cycle (*cis* converted to *trans* and again converted back to *cis*). Irradiation carried out following the first photoisomerization cycle did not change the wettability on the surface. Future work will include obtaining UV-Vis spectra of the multilayer film of mixed monolayers of 4-[(10-mercaptodecyl)oxy]pyridine-2,6-dicarboxylic acid and 4-*tert* butylbenzenethiol + Cu(II) + stilbene-4,4'-dicarboxylic acid on the gold surface and following the changes which occur upon irradiation of the films.

## References

- <sup>1</sup>. Feynman, R.P. "There's Plenty of Room at the Bottom: An Invitation to Enter a New Field of Physics" Published in *California Institute of Technology: Engineering and Science*, February, **1960**.
- <sup>2</sup>. Lee, S.M.; Koepsel, R.; Stolz, D.B.; Warriner, H.E.; Russell, A.J. *J. Am. Chem. Soc.*, **2004**, *126*, 13400.
- <sup>3</sup>. Langmuir, I. *J. Am. Chem. Soc.*, **1917**, *39*, 1848.
- <sup>4</sup>. Blodgett, K.B. *J. Am. Chem. Soc.*, **1935**, *57*, 1007.
- <sup>5</sup>. Haller, I. *J. Am. Chem. Soc.*, **1978**, *100*, 8050.
- <sup>6</sup>. Sagiv, J. *J. Am. Chem. Soc.*, **1980**, *102*, 92.
- <sup>7</sup>. Nuzzo, R.G.; Allara, D.L. *J. Am. Chem. Soc.* **1983**, *105*, 4481
- <sup>8</sup>. Whitesides G.M.; Nuzzo R.G.; Bain C.D.; Troughton E.B.; Tao Y.; Evall J. *J. Am. Chem. Soc.*, **1989**, *111*, 321
- <sup>9</sup>. Porter, M.D.; Bright, T.B.; Allara, D.L.; Chidsey, C.E.D. *J. Am. Chem. Soc.*, **1987**, *109*, 3559.
- <sup>10</sup>. Nuzzo, R.G.; Fusco, F. A.; Allara, D. L. *J. Am. Chem. Soc.* **1987**, *109*, 2358.
- <sup>11</sup>. Strong, L.; Whitesides, G.M. *Langmuir* **1988**, *4*, 546.
- <sup>12</sup>. Patai, S.; Rappaport, Z. *The Chemistry of Organic Derivatives of Gold and Sulfur*. John Wiley and Sons: New York, **1999**.
- <sup>13</sup>. Bain, C.D.; Evall, J.; Whitesides, G.M. *J. Am. Chem. Soc.* **1989**, *111*, 7155.
- <sup>14</sup>. Ulman, A.; Evans, S.D.; Shnidman, Y.; Sharma, R.; Eilers, J.E.; Chang, J. C. *J. Am. Chem. Soc.* **1991**, *113*, 1499.
- <sup>15</sup>. Pale-Grosdemange, C.; Simon, E. S.; Prime, K.L.; Whitesides, G.M. *J. Am. Chem. Soc.* **1991**, *113*, 13.
- <sup>16</sup>. Chidsey, C.E.D.; Bertozzi, C.R.; Putvinski, T.M.; Mujisce, A.M. *J. Am. Chem. Soc.* **1990**, *112*, 4301.
- <sup>17</sup>. Rowe, G.K.; Creager, S.E. *Langmuir* **1991**, *7*, 2307.

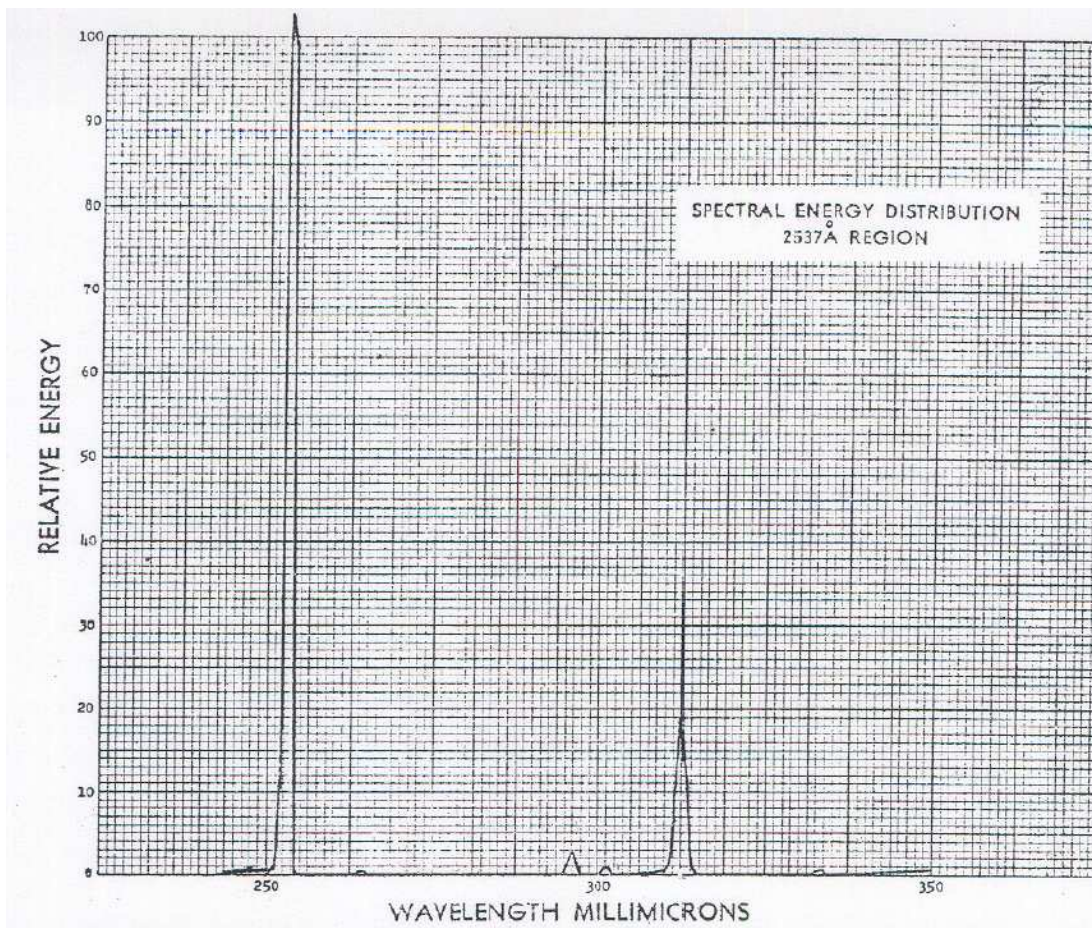
18. Hickman, J. J.; Ofer, D.; Laibinis, P.E.; Whitesides, G.M.; Wrighton, M.S. *Science* **1991**, *252*, 688.
19. Evans, D.S.; Ulman, A.; Goppert-Berarducci, K.E.; Gerenser, L. *J. Am. Chem. Soc.*, **1991**, *113*, 5866.
20. Brust, M.; Blass, P.M.; Bard, A.J. *Langmuir*, **1997**, *13*, 5607
21. McGimpsey, W.G.; MacDonald, J.C.; Cooper, C.G.F.; Soto, E.R. *J. Am. Chem. Soc.* (Comm. Ed.) **2003**, *125*, 2838
22. McGimpsey, W.G.; MacDonald, J.C.; Soto, E.R.; Cooper, C.G.F. *J. Am. Chem. Soc.* (Comm. Ed.), **2004**, *126*, 1030.
23. Graighead, H.G. *Science* **2000**, *290*, 1532.
24. Jacobs, H.O.; Tao, A.R.; Schwartz, A.; Gracias, D.H.; Whitesides, G.M. *Science* **2002**, *296*, 323.
25. Nath, N.; Chilkoti, A.; *Adv. Mater.* **2002**, *14*, 1243.
26. Abbott, S.; Ralston, J.; Reynolds, G.; Hayes, R. *Langmuir* **1999**, *15*, 8923.
27. Liu, Y.; Mu, L.; Liu, B.H.; Zhang, S.; Yang, P.Y.; Kong, J. L. *Chem. Commun.* **2004**, 1194.
28. Finklea, H. O.; Hanshew, D. D.; *J. Electroanal. Chem.* **1993**, *347*, 327.
29. Synder, R.G.; Strauss, H.L.; Elliger, C.A. *J. Phys. Chem.* **1982**, *86*, 5145.
30. Synder, R.G.; Maroncelli, M.; Strauss, H.L.; Hallmark, V.M. *J. Phys. Chem.* **1986**, *90*, 5623.
31. Nuzzo, R. G.; Dubois, L. H.; Allara, D. L. *J. Am. Chem. Soc.* **1990**, *112*, 558.
32. Anderson, M. R.; Evaniak, M. N.; Zhang, M. *Langmuir* **1996**, *12*, 2327
33. Gatin, M. R.; Anderson, M. R. *Vib. Spectrosc.* **1993**, *5*, 255.
34. Golden, W. G.; Dunn, D. S.; Overend, J. *J. Catal.* **1981**, *71*, 395.
35. Laibinis, P.E.; Bain, C.D.; Nuzzo, R.G.; Whitesides, G.M. *J. Phys. Chem.*, **1995**, *99*, 7663.
36. Chaudhury, M.K.; Whitesides, G.M. *Science*, **1992**, *256*, 1539.

- <sup>37</sup>. Laibinis, P.E.; Whitesides, G.M. *Langmuir*, **1990**, *6*, 87.
- <sup>38</sup>. Liedberg B.; Lestelius M.; Engquist I.; Tengvall P.; Chaudhury M.K.; *Colloids and Surfaces B: Biointerfaces* , **1999**, *15*,57.
- <sup>39</sup>. Bain, C. D.; Whitesides, G. M. *J. Am. Chem. Soc.* **1988**, *110*, 3665.
- <sup>40</sup>. Bain, C. D.; Whitesides, G. M. *J. Am. Chem. Soc.* **1988**, *110*, 5897.
- <sup>41</sup>. Bain, C. D.; Whitesides, G. M. *J. Am. Chem. Soc.* **1988**, *110*, 6560.
- <sup>42</sup>. Morita, T.; Kimura, S.; Kobayashi, S.; Imanishi, Y. *J. Am. Chem. Soc.*, **2000**, *122*, 2850.
- <sup>43</sup>. Li, H.; Xu, J.; *Journal of Colloid and Interface Science* **1995**, *176*, 138.
- <sup>44</sup>. Brett, A. O.; Brett C. M.; Kresak S.; Hianik T.; *Electroanalysis* **2003**, *5-6*, 15.
- <sup>45</sup>. Miller, C. J.; Cuendet, P.; Gratzel, M. *J. Phys. Chem.*,**1991**, *95*, 877.
- <sup>46</sup>. Miller, C. J.; Gratzel, M. *J. Phys. Chem.*, **1991**, *95*, 5225.
- <sup>47</sup>. Miller, C. J.; Gratzel, M. *J. Phys. Chem.* **1992**, *96*, 2657.
- <sup>48</sup>. Becka, A. M., Miller, C. J., *J. Phys. Chem.* **1993**, *97*, 6233.
- <sup>49</sup>. Xu, J., Li, H.-L., *J. Phys. Chem.* **1993**, *97*, 11497.
- <sup>50</sup>. Song, S.; Clark, R. A.; Bowden, E. F.; Tarlov, M. J.; *J. Phys. Chem.* **1993**, *97*, 6564.
- <sup>51</sup>. Laibinis, P. E.; Whitesides, G. M.; Allara, D. L.; Tao, Y.-T.; Parikh, N.; Nuzzo, R. G. *J. Am. Chem. Soc.* **1991**, *113*, 7152.
- <sup>52</sup>. Ahn, H.; Kim, M.; Sandman, D.J.; Whitten, J.E. *Langmuir* **2003**, *19*, 5303.
- <sup>53</sup>. Lee, S.; Puck, A.; Graupe, M.; Colorado, R.; Shon, Y.; Lee, R.T.; Perry, S.S. *Langmuir* **2001**, *17*, 7364.
- <sup>54</sup>. Wolf, M.O.; Fox, M. A. *Langmuir*, **1996**, *12*, 955.
- <sup>55</sup>. Quina, F. H.; Whitten, D. G. *J. Am. Chem. Soc.* **1975**, *97*, 1602.
- <sup>56</sup>. Quina, F. H.; Whitten, D. G. *J. Am. Chem. Soc.* **1977**, *99*, 877.
- <sup>57</sup>. Whitten, D. G. *J. Am. Chem. Soc.* **1974**, *96*, 594.

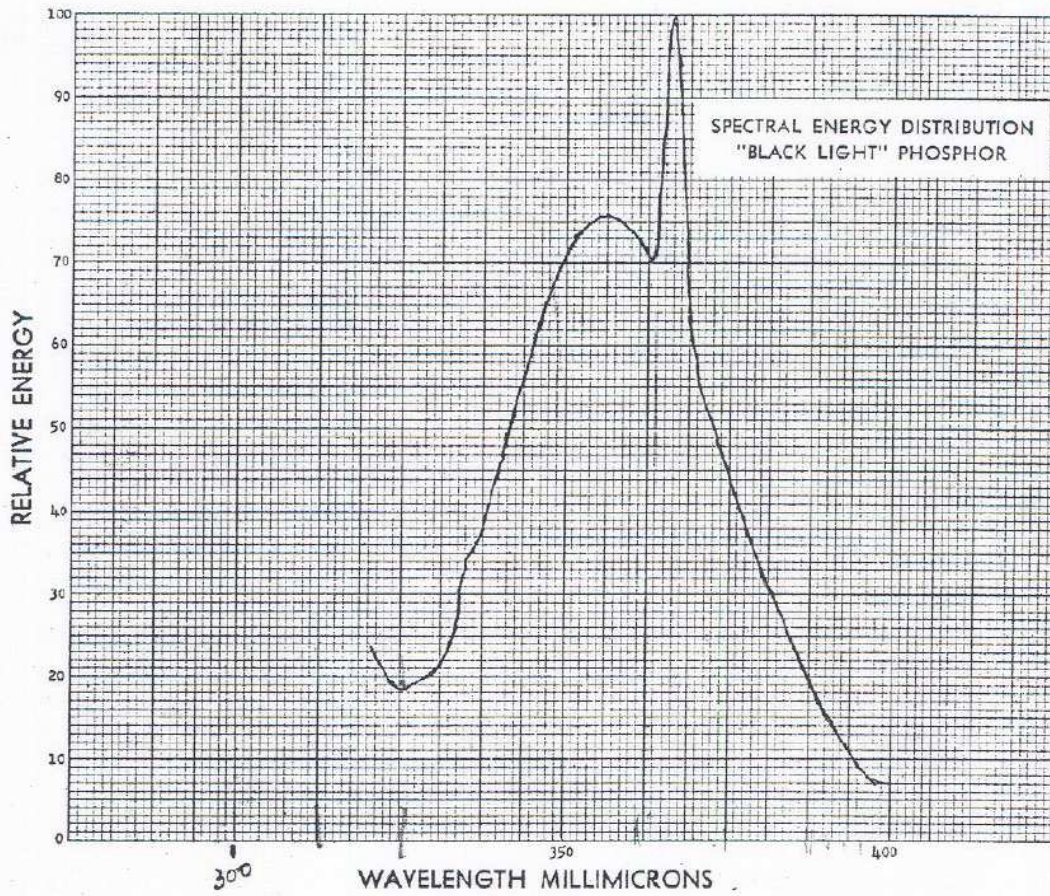
- <sup>58</sup>. Whitten, D. G. *Angew. Chem. Int. Ed. Engl.* **1979**, *18*, 440.
- <sup>59</sup>. Green, B.S.; Heller L. *J. Org. Chem* **1974**, *39*,196
- <sup>60</sup>. Hu, J.; Fox, M.A.; Zhang, J.; Liu, F. ; Kittredge K.; Whitesell J. K. *J. Am. Chem. Soc.* **2001**, *123*, 1464.
- <sup>61</sup>. Wolf, H.; Evans, S.D.; Johnson S.R.; Ringsdorf H.; Williams L.M. *Langmuir*, **1998**, *12*, 955.
- <sup>62</sup>. Stranick, S. J.; Parikh, A. N.; Tao, Y. T.; Allara, D. L.; Weiss, P. S. *J. Phys. Chem.* **1994**, *98*, 7636.
- <sup>63</sup>. Prime, K. L.; Whitesides, G. M. *Science* **1991**, *252*, 1164.
- <sup>64</sup>. Prime, K. L.; Whitesides, G. M. *J. Am. Chem. Soc.* **1993**, *115*,10714.
- <sup>65</sup>. Laibinis, P.E.; Nuzzo, R.G. ; Whitesides G.M. *J. Phys. Chem.* **1992**, *96*, 5097.
- <sup>66</sup>. Larsen, A. G.; Gothelf, K.V.; *Langmuir*, **2005**, *2*,1015.
- <sup>67</sup>. Gupta, P.; Ulman, A.; Fanfan, S.; Korniaikov, A.; Loos, K. *J. Am. Chem. Soc.* **2005**; *127*, 4.
- <sup>68</sup>. Abbott, S.; Ralston, J.; Reynolds, G.; Hayes, R. *Langmuir*, **1999**, *15*, 8923.

## Appendix A

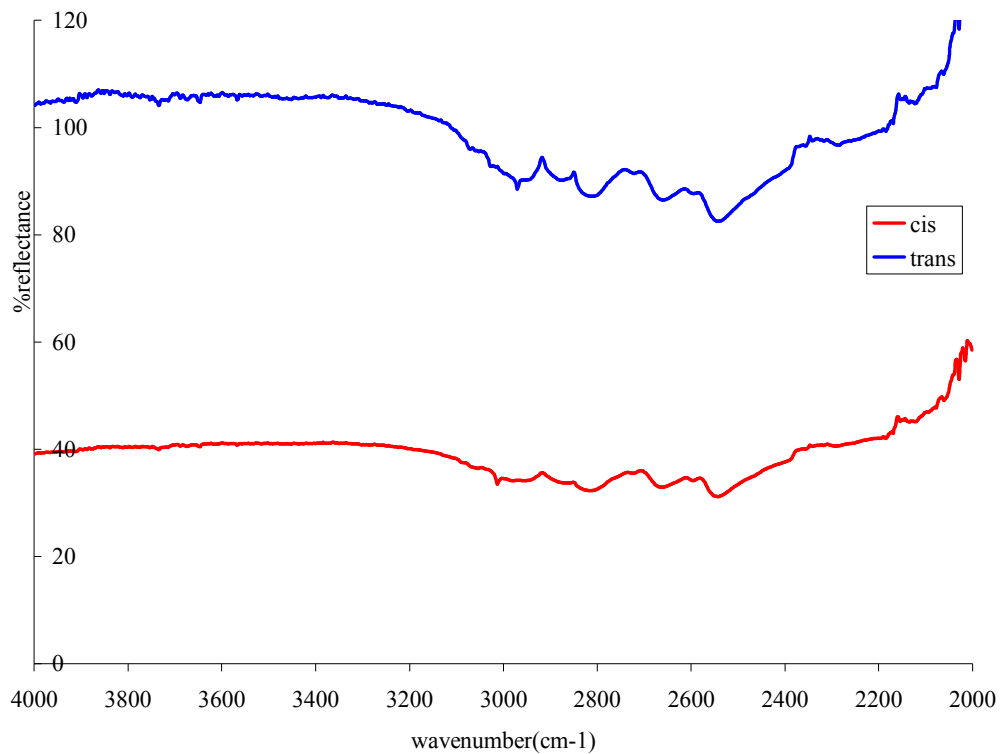
# Lamp Profile of 254nm Rayonet lamp



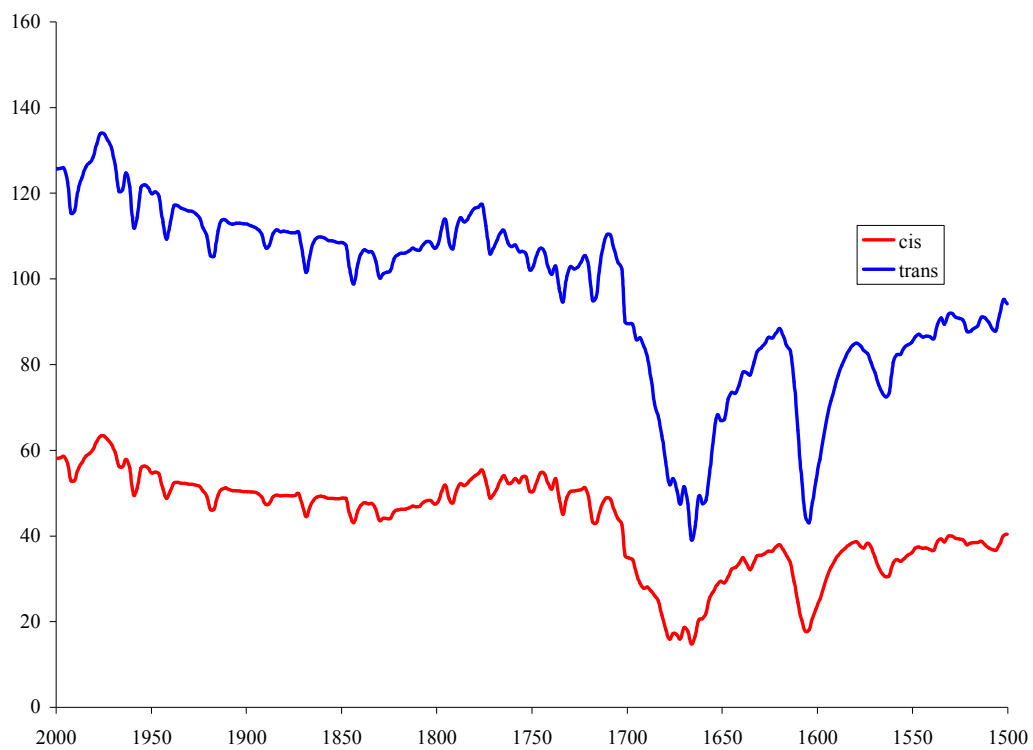
# Lamp Profile of 350nm Rayonet lamp



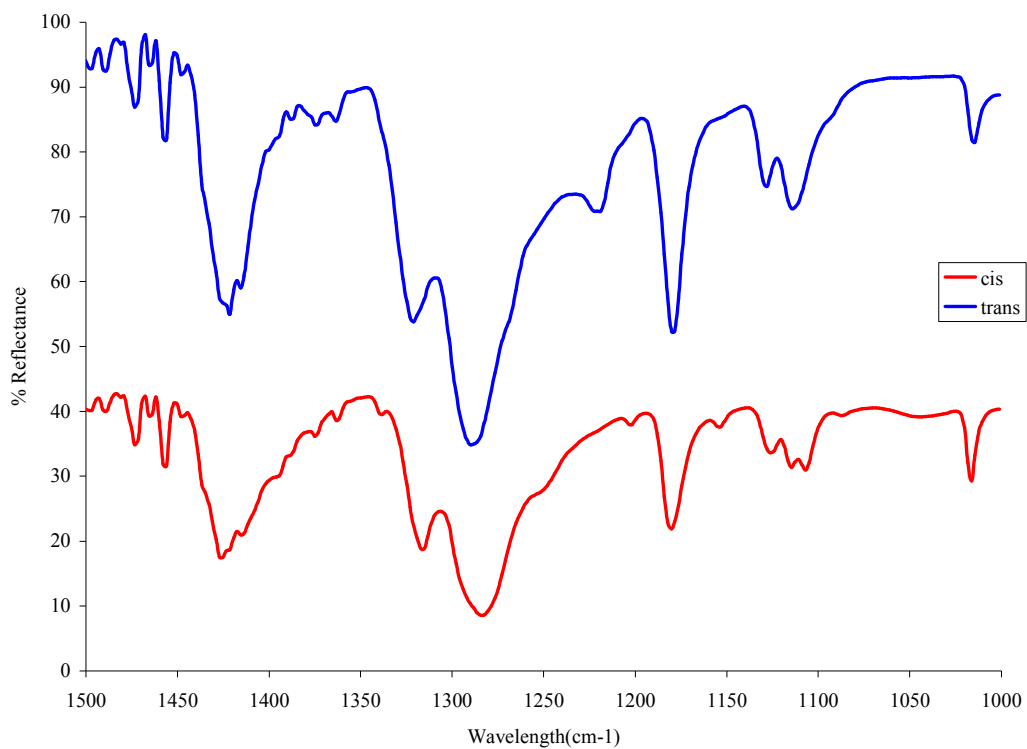
IR spectra of solid *cis* and *trans* stilbene-4,4'-dicarboxylic acid from 4000 $\text{cm}^{-1}$  to 2000  $\text{cm}^{-1}$

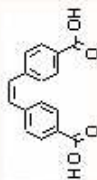


IR spectra of solid *cis* and *trans* stilbene-4,4'-dicarboxylic acid from 2000 $\text{cm}^{-1}$  to 1500  $\text{cm}^{-1}$

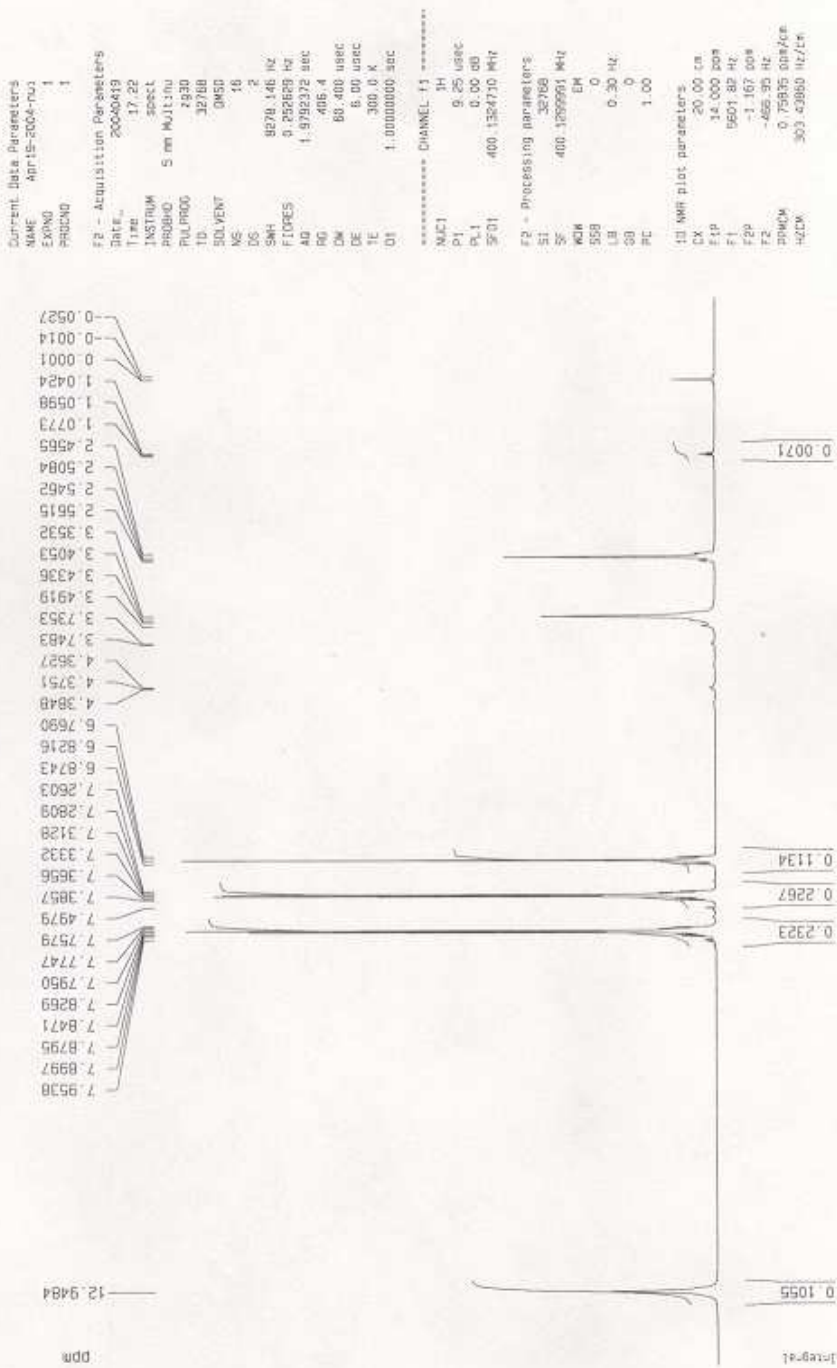


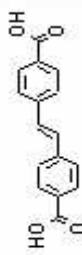
IR spectra of solid *cis* and *trans* stilbene-4,4'-dicarboxylic acid from 1500 $\text{cm}^{-1}$  to 1000  $\text{cm}^{-1}$





protected cis-stilbene-dicarboxylic acid





trans-stilbene dicarboxylic acid

Current Data Parameters  
 NAME Apr29\_2004-nu  
 EXPNO 3  
 PROCNO 1

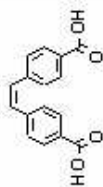
F2 - Acquisition Parameters  
 Date\_ 20040429  
 Time 17:00  
 INSTRUM spect  
 PULPROG sm Multino  
 TO 60.36  
 SOLVENT DMSO  
 NS 128  
 DS 0  
 SM 8070.146 Hz  
 FIDRES 0.176314 Hz  
 AQ 3.5684243 sec  
 RG 912.3  
 DW 60.400 usec  
 DE 5.00 usec  
 TE 300.0 K  
 D1 2.00000000 sec

\*\*\*\*\* CHANNEL f1 \*\*\*\*\*  
 NUC1 1H  
 P1 5.25 usec  
 PL1 0.00 dB  
 SFO1 400.1264710 MHz

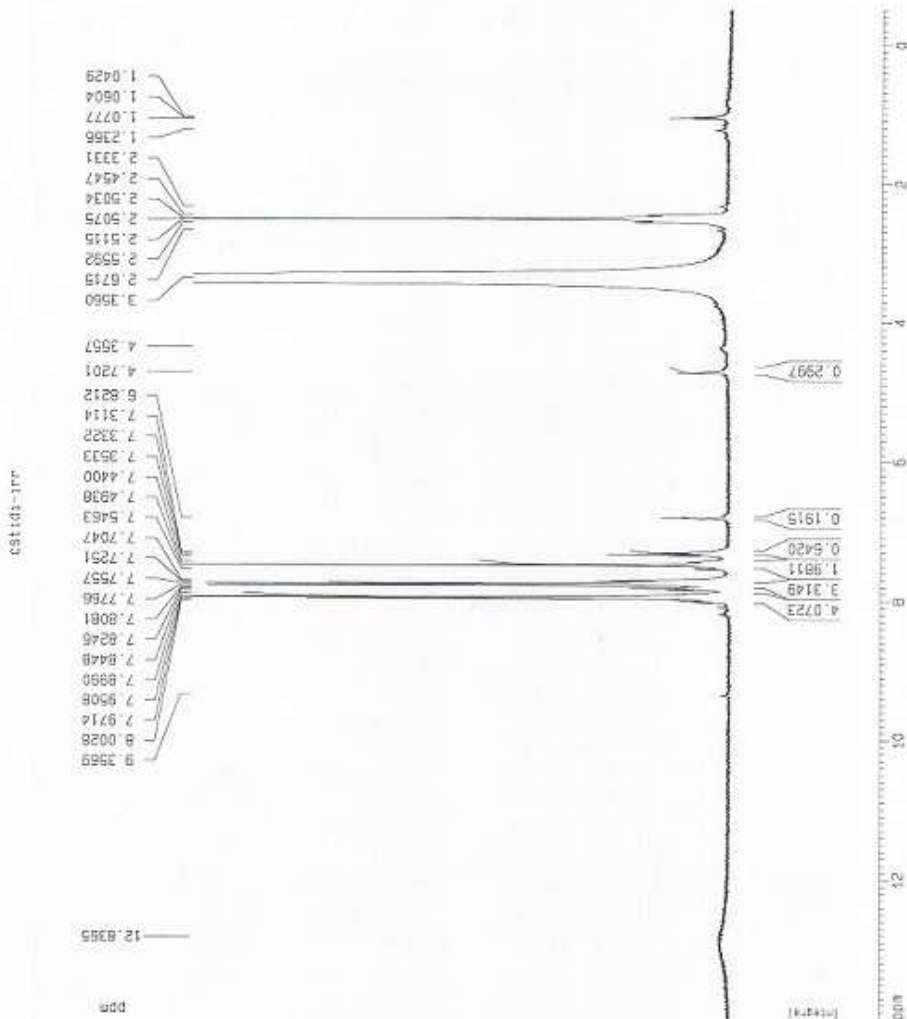
F2 - Processing parameters  
 SI 32768  
 SF 400.1300000 MHz  
 NDM DM  
 SSB 0  
 LO 0.30 Hz  
 CO 0  
 PC 1.00

10 MHz plot parameters  
 CX 20.00 cm  
 FFO 34.500 gpm  
 F1 9801.88 Hz  
 F2 -1.816 gpm  
 F2 -847.43 Hz  
 PPM 0.86560 spm/cg  
 AQCM 300.46478 m/z/cg





Irradiated



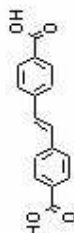
Current Data Parameters  
 NAME JLN05-004-mus  
 CINO 10  
 PROCAM 1

F2 - Acquisition Parameters  
 Date\_ 20040529  
 Time 23.20  
 INSTRUM spect  
 PROBD 5 mm Multinu  
 PU\_FID0 7530  
 TD 32768  
 SOLVENT DMSO  
 NS 16  
 DS 2  
 SWH 8270.446 Hz  
 FIDRES 0.254639 Hz  
 AQ 1.9792372 SEC  
 RG 645  
 DN 60.000 us/cp  
 DE 6.00 us/cp  
 TE 300.2 K  
 TC 1.00000000 sec

\*\*\*\*\* CHANNEL f1 \*\*\*\*\*  
 NUC1 H1  
 IN1 0.25 us/cp  
 IN2 0.00 us  
 SF01 400.1300710 MHz

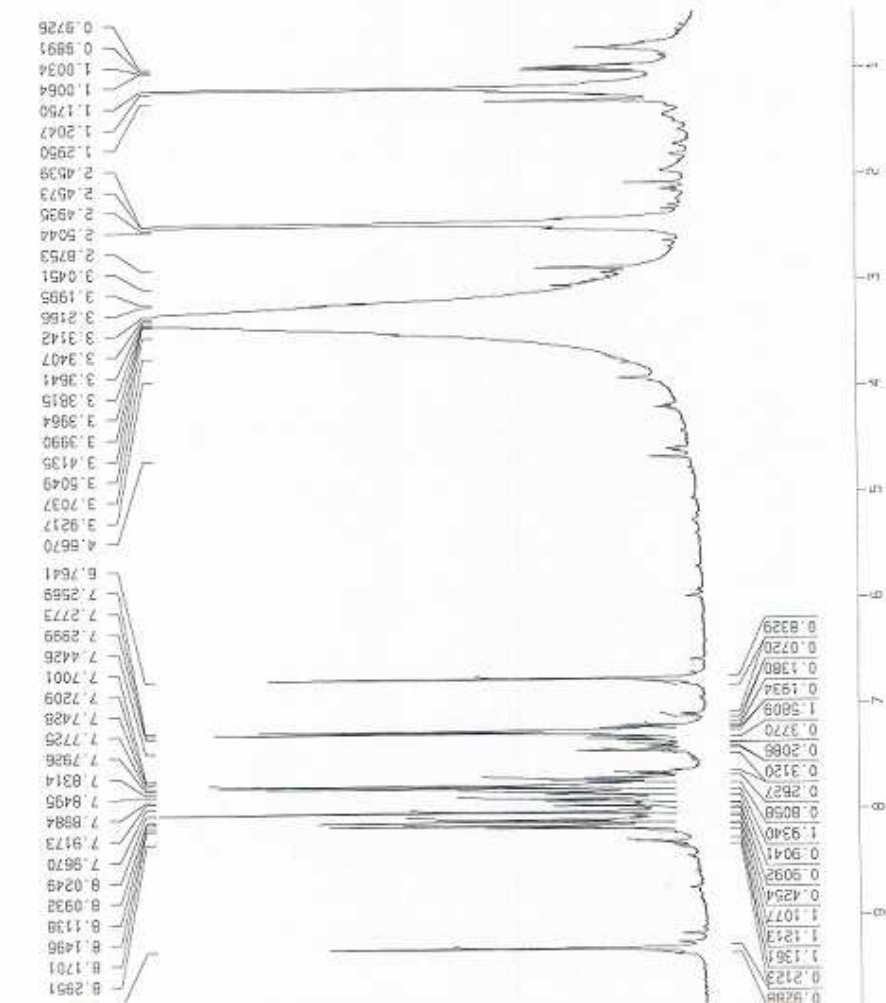
F2 - Processing parameters  
 SI 32768  
 SF 400.1300000 MHz  
 AQ 1.9792372  
 RG 645  
 DN 60.000 us/cp  
 DE 6.00 us/cp  
 TE 300.2 K  
 TC 1.00

1D NMR plot parameters  
 CX 20.00 cm  
 FID 14.000 gpm  
 F1 5001.82 Hz  
 F2 -0.500 gpm  
 F2 -200.07 Hz  
 PWDW 0.72500 gpm/cm  
 ZCON 210.09424 Hz/cm



Irradiated

trans-1H<sup>1</sup>



Current Data Parameters  
 NAME Jun14-2004 (u)  
 EXPO 1  
 PWD20 1

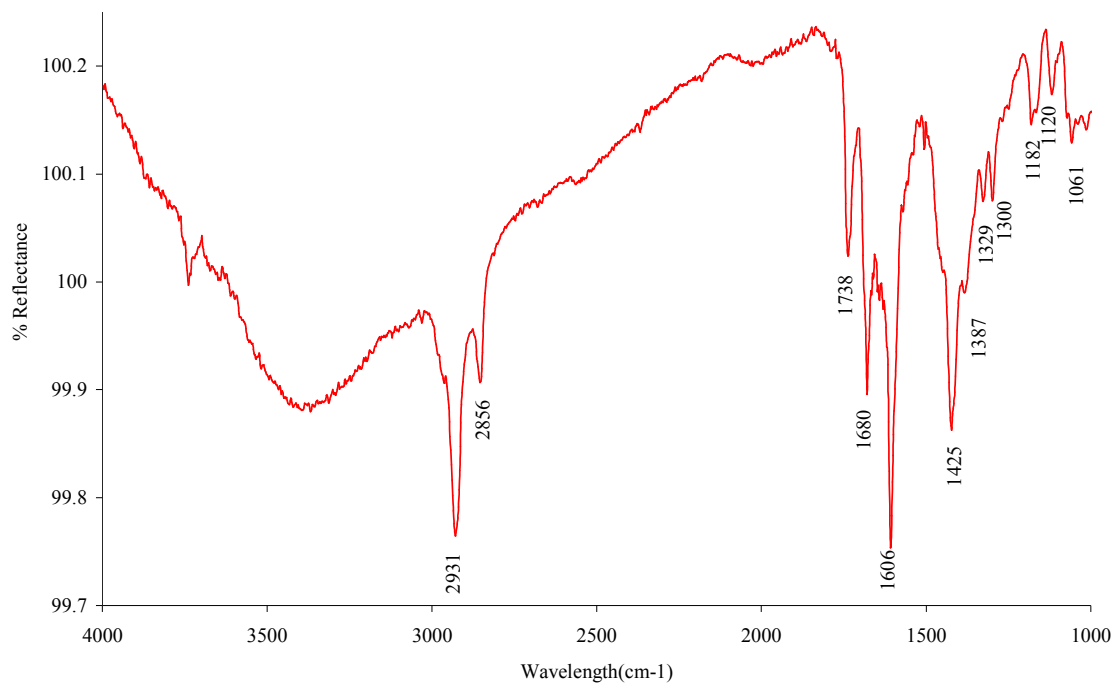
FR - Acquisition Parameters  
 Date\_ 20040514  
 Time\_ 15:32  
 INSTRUM 800CL  
 ANALYST  
 PAPER04 5 mm N11-904  
 CAL-PRG 4330  
 ID 65006  
 SOLVENT DM50  
 NS 108  
 DS 0  
 SH 8278.146 Hz  
 FIDRES 0.121634 Hz  
 AI 3.9984803 30%  
 RS 362  
 DW 65.460 uSec  
 DE 6.00 uSec  
 TE 349.0 K  
 D1 2.10000000 sec

\*\*\*\*\* CHANNEL 11 \*\*\*\*\*  
 MFC1 5H  
 P1 9.25 uSec  
 FL1 0.00 65  
 SF01 400.1324710 MHz

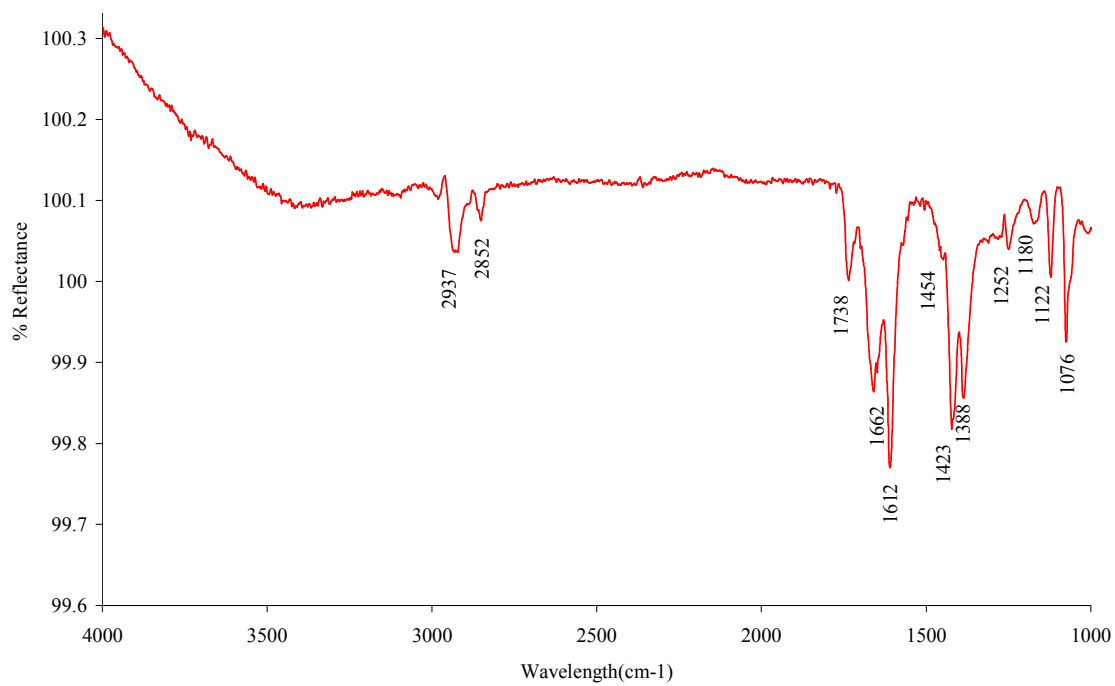
F2 - Processing parameters  
 S1 32768  
 SF 400.1300195 MHz  
 NPM 0  
 LN 0  
 SUB 0  
 LO 0.30 Hz  
 GB 0  
 PC 1.00

10 MHz plot parameters  
 DK 20.00 CH  
 FSP 10.182 DPH  
 F1 4074.24 Hz  
 F2P 0.456 DPH  
 F2 182.58 Hz  
 POW0W 0.48030 DPH/Hz  
 MODW 194.10257 Hz/CH

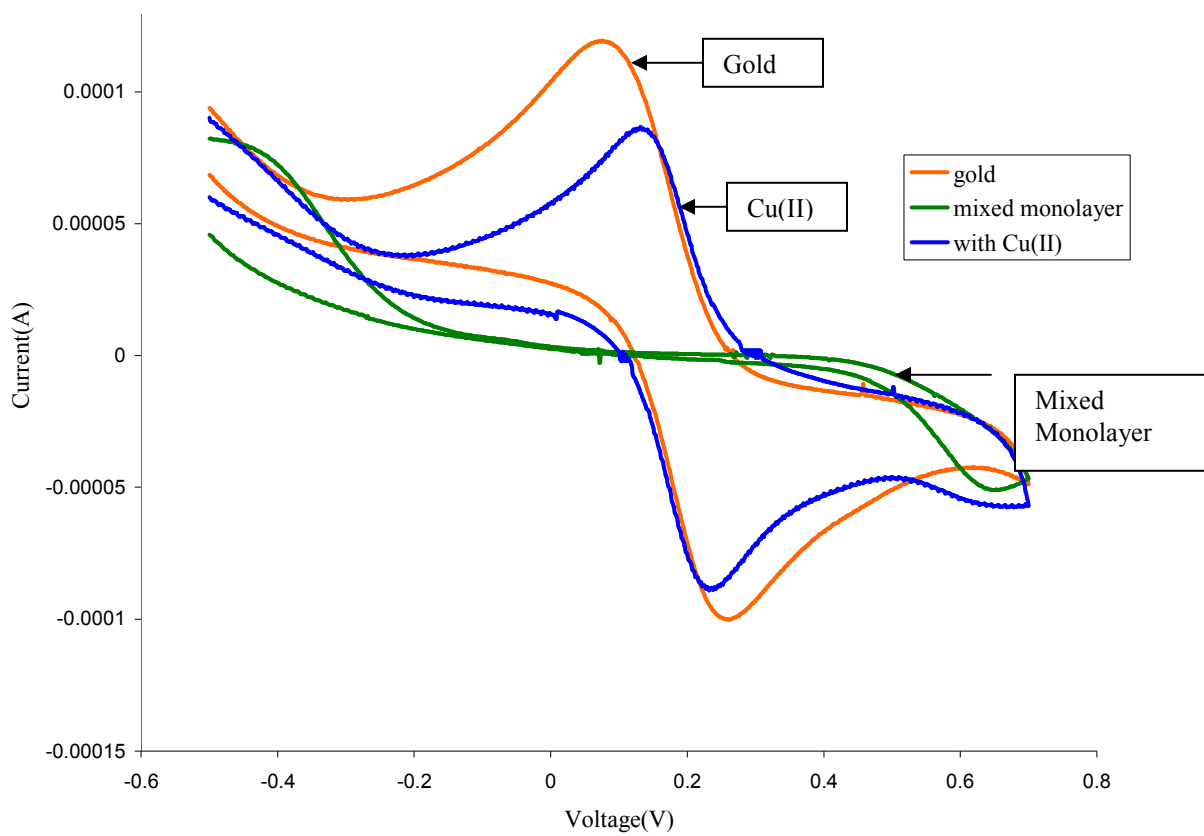
IR of Film III



IR of Irradiated Film III



Cyclic voltammograms obtained for bare gold, mixed monolayer (0.7mM mercaptoundecanoic acid and 0.3 mM dodecanethiol) on gold and Cu/mixed monolayer on gold



Cyclic voltammograms obtained for Cu(II) on mixed monolayer and *cis* stilbene-4,4'-dicarboxylic acid on Cu(II)

